



The stability of Adenoviral and mRNA based COVID-19 vaccines and the potential of HSA

A research paper/ review article submitted to The University of Nottingham in partial fulfilment of the requirements for the degree of Master of Research in Industrial Physical Biochemistry

MRes Industrial Physical Biochemistry

Khalil Mustafa Khalil Abu Hammad ID 20214336

Supervised by Professor Stephen E. Harding

Contributors: Judith Wayte, Phil Morton, Jason Cameron and Eleonora Cerasoli

University of Nottingham
National Centre for Macromolecular Hydrodynamics
School of Biosciences, Sutton Bonington
Loughborough, Leicestershire
LE12 5RD, United Kingdom
July 2021

Word count (Review paper/ Abstract): 5504 / 248

Key words: Adenoviral vector, mRNA, SARS-COV-2 virus, COVID-19 vaccine stability and human serum albumin

LIST OF CONTENTS

Abstract	IV
Abbreviations	V
CHAPTER 1 {The model of stabilised COVID-19 vaccine: Adenoviral vector platform}	
1.1 Introduction.....	2
1.1.1 Introduction to Oxford/AstraZeneca COVID-19 vaccine produced using Adenoviral vector platform.....	3
1.1.2 Introduction to Janssen COVID-19 vaccine made using Adenoviral vector platform.....	4
1.2 Oxford/AstraZeneca COVID-19 vaccine	5
1.2.1 The content, storage conditions and the physical state of the formulation.....	5
1.3 Janssen COVID-19 vaccine	7
1.3.1 The content, storage conditions and the physical state of the formulation.....	7
1.4 The strengths of Adenoviral vector platform.....	8
1.5 The weaknesses of Adenoviral vector platform.....	9
1.6 Characterisation techniques for the Oxford/AstraZeneca and Janssen platform.....	9
1.7 Adenoviral vector platform conclusion.....	10
CHAPTER 2 {The model of un-stabilised COVID-19 vaccine: mRNA platform}	
2.1 Introduction.....	12
2.1.1 Introduction to Pfizer/BioNTech COVID-19 vaccine made using mRNA platform.....	12
2.1.2 Introduction to Moderna COVID-19 vaccine made using mRNA platform.....	13
2.2 Pfizer/BioNTech COVID-19 vaccine.....	14
2.2.1 The content, storage conditions and the physical state of the formulation.....	14
2.3 Moderna COVID-19 vaccine	16
2.3.1 The content, storage conditions and the physical state of the formulation.....	16
2.4 The strengths of the mRNA platform	18
2.5 The weaknesses of the mRNA platform	18
2.6 Characterisation techniques for the Pfizer/BioNTech and Moderna platform.....	19
2.7 Problems of the mRNA platform including its instability	20
2.8 The application of the human serum albumin as a stabiliser for mRNA vaccine platform.....	20

2.8.1 Introduction.....	20
2.8.2 The structure-function relationship of human serum albumin	21
2.9 The interaction of human serum albumin for stabilising tRNA with a potential for mRNA platform.....	22
2.10 mRNA platform conclusion.....	23
CHAPTER 3 {Concluding Remarks and Perspectives}	25
List of references.....	27

Acknowledgments

It is my pleasure to conduct this research at the University of Nottingham, and I want to thank all the contributors for this work. Special thanks to my supervisor Prof. Dr Stephen E. Harding and my academic consultant Dr Judith Wayte for their guidance and invaluable support during my journey in this research.

Huge thanks to Albumedix biopharmaceutical company, especially Dr Phil Morton, Jason Cameron and Dr Eleonora Cerasoli for their inputs, suggestions, and feedback.

Finally, I am grateful to my lovely father, Mustafa Abu Hammad and my mother Sana Barqawi, who have funded this research and gave me all the support that I need to complete my Master of Research degree.

Abstract

At the end of 2019, the SARS-COV-2 virus was observed to cause respiratory disease, and it is responsible for the high number of patients admitted to hospital. Many biopharmaceutical / biotechnology companies have started manufacturing vaccines that can prevent the SARS-COV-2 virus. An important issue is COVID-19 vaccine stability, one of the most frequently stated problems faced through vaccination programs particularly in the high temperatures low-income countries. Along with cost, availability, and delivery – stability makes delivery simple. This review analyses the characteristics of the two common groups of COVID-19 vaccines – Adenovirus based (such as the Oxford/AstraZeneca and Janssen vaccines) and mRNA based (such as Pfizer/BioNTech and Moderna) – and in particular the potential application of human serum albumin (HSA) as a stabiliser for the mRNA COVID-19 platform.

From the stability point of view, while the Adenoviral vector-based vaccines can be stabilised and stored at 2–8 °C range yielding 6 months shelf-life, the mRNA-based vaccines have to be stored at much lower temperatures, limiting their distribution to the higher temperature regions. This emphasise the importance of research into formulation solutions, such as the use of excipients like human serum albumin, to improve these products stability and, therefore facilitate vaccination programs without the need for cold chain storage. The availability of these vaccines to low-income countries would have a major role in lowering the cases of COVID-19 infections. In future investigations, it is possible to look at different unstable COVID-19 platforms by applying new technologies for making a stabilise vaccine.

Abbreviations

<i>Ad26</i>	Adenovirus type 26
<i>AEX-HPLC</i>	Anion exchange high performance liquid chromatography
<i>ALC-0159</i>	2[(polyethylene glycol)-2000]-N,N- ditetradecylacetamide
<i>ALC-0315</i>	(4-hydroxybutyl) azanediyl) bis(hexane-6,1-diyl) bis (2-hexyldecanoate)
<i>AVV</i>	Adenoviral Vector
<i>BNT162b2</i>	Pfizer/BioNTech vaccine platform
<i>ChAdOx1</i>	Chimpanzee adenovirus-vectored vaccine
<i>COVID-19</i>	Coronavirus disease
<i>Cov2.S</i>	Encoding SARS-COV-2 spike glycoprotein
<i>Cys34</i>	Cysteine 34
<i>ddPCR</i>	Droplet Digital polymerase chain reaction
<i>DNA</i>	Deoxyribonucleic acid
<i>DSPC</i>	1,2-Distearoyl-sn-glycero-3-phosphocholine
<i>dsRNA</i>	Double-stranded RiboNucleic Acid
<i>ELISA</i>	Enzyme-linked Immunosorbent Assay
<i>HBCD</i>	2-hydroxypropyl- β -cyclodextrin
<i>HEK</i>	Human embryonic kidney
<i>HSA</i>	Human serum albumin
<i>ID-PCR</i>	Identity polymerase chain reaction
<i>kDa</i>	Kilodaltons
<i>LAV</i>	Live Attenuated Virus
<i>LC-UV/MS</i>	Liquid Chromatography–Ultraviolet/Mass Spectrometry
<i>LNP</i>	Lipid nanoparticle
<i>mg</i>	Milligram
<i>mRNA</i>	Messenger RiboNucleic Acid
<i>mRNA-1273</i>	Moderna vaccine platform
<i>nCoV-19</i>	Expressed SARS-CoV-2 spike protein
<i>NGS</i>	Next Generation Sequencing
<i>PCR</i>	Polymerase chain reaction

<i>PEG</i>	Polyethylene glycol/macrogol
<i>PEG2000-DMG</i>	1,2-Dimyristoyl-rac-glycero-3-methoxypolyethylene glycol-2000
<i>QPA</i>	Quantitative PCR based potency assay
<i>qPCR</i>	Quantitative polymerase chain reaction
<i>RNA</i>	Ribonucleic acid
<i>RP-HPLC</i>	Reversed phase high performance liquid chromatography
<i>RP-UPLC</i>	Reversed-phase ultra-high-performance chromatography
<i>RT-PCR</i>	Reverse transcription polymerase chain reaction
<i>SARS-COV-2</i>	Sever Acute Respiratory Syndrome Coronavirus 2
<i>S protein</i>	Spike protein
<i>TGE-ELISA</i>	Transgene expression enzyme-linked immunosorbent assay
μg	Microgram
<i>UTR</i>	Untranslated region
<i>UV spectroscopy</i>	Ultraviolet spectroscopy
<i>VLP</i>	Virus-Like Particle
<i>VP-qPCR</i>	Viral particle-quantitative polymerase chain reaction
<i>VVr + APC</i>	Viral Vector replicating + Antigen Presenting Cells
<i>VVr</i>	Viral Vector replicating
<i>VVnr + APC</i>	Viral Vector non-replicating + Antigen Presenting cells
<i>VVnr</i>	Viral Vector non-replicating
<i>WHO</i>	World Health Organization

CHAPTER 1

The model of stabilised COVID-19 vaccine: Adenoviral vector platform

Human pathogens identified as Coronaviruses (CoV) have been known since the 1960s (Kahn and McIntosh 2005). At the end of 2019, in Wuhan Hubei China, Severe Acute Respiratory Syndrome Coronavirus 2 (SARS-COV-2) was observed causing pneumonia among patients (Guo et al. 2020; Krammer 2020; Tian et al. 2020). The SARS-COV-2 virus is responsible for the current pandemic (Guo et al. 2020; Krammer 2020; Tian et al. 2020). The Latin name of ‘corona’ means halo or crown. Indeed, the surface characteristics of the virion have a crown-like shape in appearance under the electron microscope (European Centre for Disease Prevention and Control 2021). The SARS-COV-2 is an enveloped virus (Huang et al. 2020; Qamar et al. 2020) with 65 –125 nm in diameter, and it contains single-stranded RNA (Astuti and Ysrafil 2020).

Since the outbreak, there has been a huge attempt worldwide to develop COVID-19 vaccine as a response to Coronaviruses pandemic. Its development is a crucial approach, which in a role can alleviate the burdens of the virus on society, economy and public health (Krammer 2020). According to the World Health Organisation (2021e) report, there are 10 candidate approaches of “platforms” in the clinical trial phase, which can work against the SARS-COV-2 virus. These are diverse and based on a variety of approaches such as: Deoxyribonucleic acid, Protein Subunits, Inactivated Virus, Virus-Like Particle (VLP), Live Attenuated Virus (LAV), Viral Vector replicating with the Antigen Presenting Cells (VVr + APC), Viral Vector non-replicating with the Antigen Presenting Cells (VVnr + APC), Viral Vector replicating (VVr), Viral Vector non-replicating (VVnr) and Ribonucleic acid.

One of the key important aspects of the COVID-19 vaccine platforms is stability, which can be a challenge for some biopharmaceutical companies. The cold chain storage requirements for the COVID-19 vaccine cause a logistic issue (World Health Organisation 2021g), which affects the immunisation programme quality, especially in low-income countries due to the low-temperature control (Park et al. 2021).

Albumedix is a Nottingham based biopharmaceutical company which manufactures a recombinant version of human serum albumin (HSA) protein, which is used to stabilise a wide range of active pharmaceutical ingredients and biopharmaceuticals such as peptides, proteins, vaccines and is also used in cell therapy processing. Human serum albumin is a well-known excipient and is used for a large number of regulatory-approved pharmaceuticals worldwide. This review will consider the current published knowledge around selected COVID-19 vaccine platforms. We will first show the model of stabilised COVID-19 vaccine for the Adenoviral Vector platform such as Oxford/AstraZeneca and Janssen. Then, we will highlight the model of un-stabilised COVID-19 vaccine for the mRNA platform such as Pfizer/BioNTech and Moderna. Finally, we will discuss the potential application of human serum albumin as a potential stabiliser for vaccines in general and for the mRNA platform in particular.

1.1 Introduction

Adenoviral vector (AVV) has emerged as a powerful platform that has been employed against infectious diseases (Guo et al. 2018). It is a diverse family of viruses that belongs to more than 50 serotypes called adenoviridae (Singh et al. 2019). In mammalian hosts, it can induce adaptive and innate immune responses (Tatsis and Ertl 2004). In 1953, Rowe and colleagues were the first to discover the AVV platform (Rowe et al. 1953). Additionally, the AVV can be genetically modified with foreign antigens, which can elicit T cells and specific antibody responses in hosts (Guo et al. 2018). In Cheng et al. (2015) article, it was shown that the AVV is a double-stranded DNA virus, non-enveloped and icosahedral in shape, which can infect broadly both the non-human and human primates' vertebrates.

Nowadays, there has been an increasing interest in using AVV as a platform against the SARS-COV-2 virus. This chapter will emphasise the Oxford/AstraZeneca and Janssen AAV platforms, which are examples of stabilised AAV platform.

1.1.1 Introduction to Oxford/AstraZeneca COVID-19 vaccine produced using Adenoviral vector platform

The ChAdOx1 nCoV-19 vaccine is manufactured by the University of Oxford and AstraZeneca, a UK pharmaceutical company. Two methods are used in AVV platform manufacturing: the replication-competent and incompetent vectors (Figure 1).

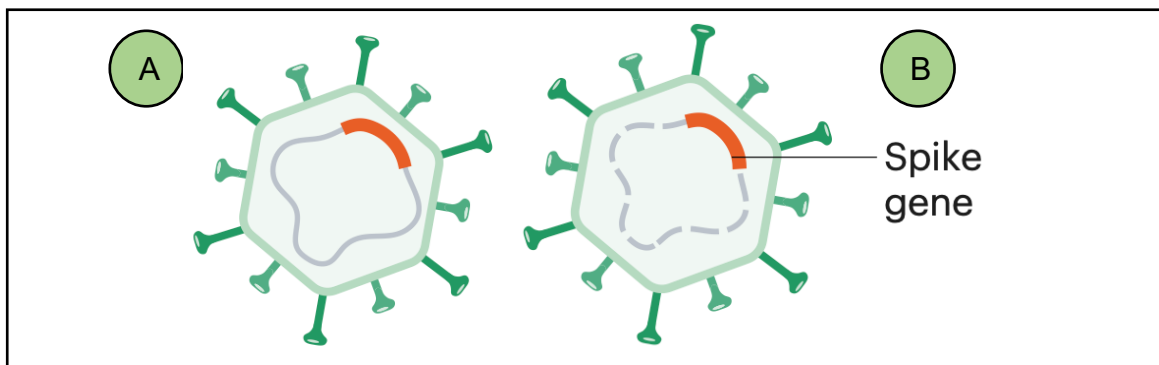


Figure (1): Adenoviral vector used two methods in vaccine manufacturing by inserting the spike gene. (A) Replication-competent vector. (B) Replication-incompetent vector - adapted from Krammer (2020 p.520 fig.3).

The replication-competent vector (Figure1, A) expresses the virus spike protein and propagates in the vaccinated cells. However, the replication-incompetent vector (Figure1, B) articulates the virus spike protein but cannot propagate in the vaccinated cells. Accordingly, ChAdOx1 nCoV-19 vaccine used the replication-incompetent vector, which is based on the engineered chimpanzee Adenoviral vector virus to express the SARS-CO-2 virus spike protein; by disabling the virus from replication via deletions in the genomic parts (Krammer 2020).

1.1.2 Introduction to Janssen COVID-19 vaccine made using Adenoviral vector platform

The Ad26.Cov2.S vaccine is manufactured by Janssen Pharmaceutical Companies. The Ad26.Cov2.S is a recombinant viral vector platform that uses human adenovirus to express the SARS-COV-2 virus spike protein (World Health Organisation 2021b). Indeed, it referred to a species D from adenovirus type 26 (Ad26), and it is one of the most common replication-incompetent vectors (Figure1, B) (Khare et al. 2011; Pinschewer 2017; World Health Organisation 2021b). In the European Medicines Agency (2021c) report, it reported that the Ad26.Cov2.S vaccine encodes the SARS-COV-2 spike gene inside the $\Delta E1A/E1B$ region, encompassing stabilising modifiers after deletions in the E1 region (Figure 2). Additionally, part of the E3 region was removed, which is $\Delta E3$, to create a sufficient space in the viral genome to insert the SARS-COV-2 spike gene. Once the Ad26.Cov2.S vaccine is injected, the cells start expressing the spike gene on the cell surfaces for the immune response.

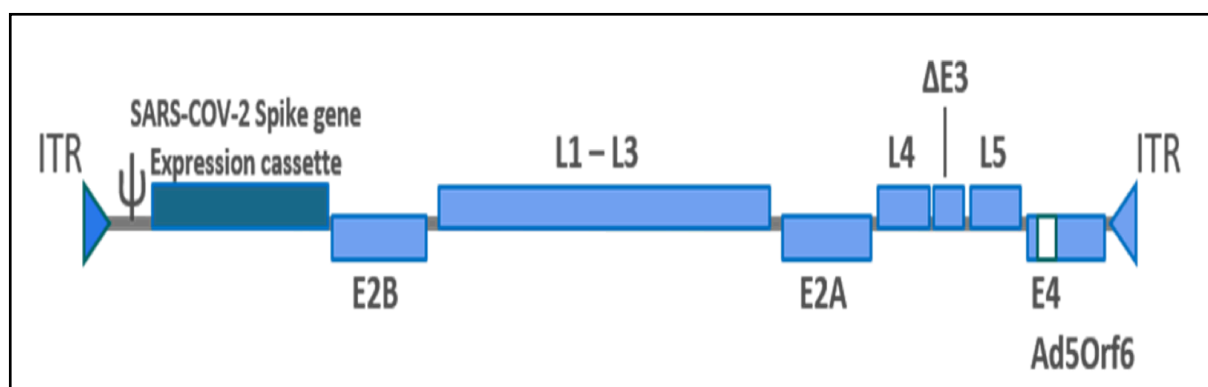


Figure (2): Adenoviral vector type 26 encoding the SARS-COV-2 virus in the $\Delta E1A/E1B$ region including stabilising modifications – copied from European Medicines Agency (2021c p.20 fig.2).

1.2 Oxford/AstraZeneca COVID-19 vaccine

The Oxford/AstraZeneca COVID-19 vaccine (ChAdOx1 nCoV-19) prevents SARS-COV-2 virus through the activation of an individual's immune system – natural defences. This vaccine has been approved in many countries for use in those aged 18 years and older (Medicines & Healthcare products Regulatory Agency 2021d).

1.2.1 The content, storage conditions and the physical state of the formulation

The ChAdOx1 nCoV-19 vaccine produced using genetically modified organisms of the human embryonic kidney (HEK) 293 cells (Medicines & Healthcare products Regulatory Agency 2021a). Each dose of ChAdOx1 nCoV-19 vaccine contains viral particle and excipients as stated in Table 1.

Table 1: The content of Oxford/AstraZeneca COVID-19 vaccine formulation with their reported concentrations (Medicines & Healthcare products Regulatory Agency 2021a).

*It is a recombinant, chimpanzee adenovirus vector.

Oxford/AstraZeneca COVID-19 (ChAdOx1 nCoV-19) vaccine formulation		
1 dose (0.5 ml)	The content of the formulation.	Concentrations per dose.
Viral particle	ChAdOx1-S*.	5×10^{10} viral particles.
Other excipients	1. L-histidine.	Not reported.
	2. L-histidine hydrochloride monohydrate.	Not reported.
	3. Magnesium chloride hexahydrate.	Not reported.
	4. Polysorbate 80 (E433).	<100 µg per dose (Turner et al. 2021).
	5. Ethanol 95%.	2 mg (AstraZeneca 2021).

	6. Sucrose.	Not reported.
	7. Sodium chloride.	<1 mmol sodium \approx 23 mg/0.5 ml dose + sodium-free (AstraZeneca 2021).
	8. Disodium edetate dihydrate.	Not reported.
	9. Water for injections.	Not reported.

The content of Oxford/AstraZeneca formulation has some different viral particles and other excipients from Janssen such as L-histidine and L-histidine hydrochloride monohydrate, which provides buffering; magnesium chloride hexahydrate and disodium edetate dihydrate acting as a stabiliser; sucrose acts as tonicifier/stabiliser (European Medicines Agency 2021b). In contrast to Oxford/AstraZeneca formulation, however, Janssen formulation used citric acid monohydrate and trisodium citrate dihydrate as a buffering agent; HBCD is used instead of magnesium chloride hexahydrate and disodium edetate dihydrate in the Oxford/AstraZeneca formulation as a stabiliser.

The knowledge of ChAdOx1 nCoV-19 vaccine storage conditions and the physical state is important for better understanding of AVV stability. Most vaccines should be kept in the refrigerator from production until the use due to their thermosensitivity. Ensuring vaccine stability is important for conducting immunisation programs (Clénet 2018). Furthermore, Oxford/AstraZeneca formulation can be stored within the 2 –8 °C range without the need to be kept at freezing temperatures. Its formulation is impacted by light; therefore, the vials should be kept in the outer carton. In contrast, Oxford/AstraZeneca formulation can be stored within the 2-25 °C range during its use. Once the first dose is withdrawn the other doses should be used within 6 hours (Medicines & Healthcare products Regulatory Agency 2021a).

The long-term storage of ChAdOx1 nCoV-19 vaccine substance was revealed to be adequate, and the proposed shelf-life was 6 months (Medicines & Healthcare products Regulatory Agency 2021d). The vaccine colour showed colourless to a slightly opalescent solution (World Health Organisation 2021b).

1.3 Janssen COVID-19 vaccine

The Janssen COVID-19 vaccine (Ad26.Cov2.S) provokes neutralising antibodies in healthy individuals and has been approved for use among 18 and 55 years old (World Health Organisation 2021c).

1.3.1 The content, storage conditions and the physical state of the formulation

The Janssen company summarised important information about AD26.COVS.S formulation with their concentrations (Table 2).

Table 2: The content of AD26.COVS.S formulation with their reported concentrations (World Health Organisation 2021c).

Janssen COVID-19 vaccine (AD26.COVS.S) formulation		
1 dose (0.5 ml)	The content of the formulation.	Concentrations per dose.
Viral particle	AD26.COVS.S viral particles.	5×10^{10} viral particles.
Other excipients	1- Polysorbate 80 (E433).	0.16 mg/dose (Banerji et al. 2021; Janssen Pharmaceutical Companies 2021).
	2- Ethanol 95%.	2.04 mg (Janssen Pharmaceutical Companies 2021).
	3- Sodium chloride.	2.19 mg (Janssen Pharmaceutical Companies 2021).
	4- Citric acid monohydrate.	0.14 mg (Janssen Pharmaceutical Companies 2021).
	5- Trisodium citrate dihydrate	2.02 mg (Janssen Pharmaceutical Companies 2021).
	6- 2-hydroxypropyl- β -cyclodextrin (HBCD).	25.50 mg Janssen Pharmaceutical Companies 2021).
	7- Sodium hydroxide.	Not reported.
	8- Hydrochloric acid.	Not reported.

The content of Janssen formulation has the same viral particles and other excipients from Oxford/AstraZeneca platform such as sodium chloride, ethanol 95% and polysorbate 80 (E433) (AstraZeneca 2021; Janssen Pharmaceutical Companies 2021; Turner et al. 2021).

The awareness of AD26.COV2.S formulation storage conditions and physical state is important for a better understanding of AVV stability. Currently due to the COVID-19 pandemic, there is a desire for a convenient and rapid distribution chain with suitable storage of the formulation. The convenient and rapid distribution chain could improve the COVID-19 vaccine stability profile, which can lead the formulation to be stored at the refrigerator with a low cost of manufacturing. It also minimises the logistic barriers that make it more accessible to patients (Crommelin et al. 2021b). Its shelf life is provided at -20°C for 2 years but it can be stored within $2-8^{\circ}\text{C}$ range for up to 3 months with no need for reconstitution. If the vaccine is thawed, it should not be re-frozen again. Nevertheless, the light might affect vaccine formulation and the vials should be kept in the outer carton; whereas the colour of the vaccine product is colourless to slightly yellow, and it is an opalescent suspension in terms of the physical state (World Health Organisation 2021c).

1.4 The strengths of Adenoviral vector platform

In vaccine development, each platform has strengths and weaknesses. This part intends to discuss the Adenoviral vector (AVV) strengths. Adenoviral vectors can affect the immune system, and their effects induce robust humoral and cellular immunity pathways against the introduced antigens (Haque and Pant 2020; Stanberry and Strugnell 2011). In regards to drug delivery, it can facilitate oral delivery through its application to the mucosal surface (Stanberry and Strugnell 2011). Regarding its production, the AVV can be easily engineered (Stanberry and Strugnell 2011). Concerning its genetic expression, it has long-term gene expression (Haque and Pant 2020).

1.5 The weaknesses of Adenoviral vector platform

The Adenoviral vector (AVV) platform has weaknesses in vaccine development. In regards to immunity, the AVV has a potential for both lack of attenuation and over attenuation. The pre-existing vector antibodies decrease the efficacy of the AVV and cause a misdirection for the immune response (Haque and Pant 2020; Rerks-Ngarm et al. 2009; Stanberry and Strugnell 2011). It limits the subsequent dose from its specific response (Stanberry and Strugnell 2011). In immunocompromised hosts, the Adenoviral vector causes diseases due to the viruses' recombination. According to Stanberry and Strugnell (2011) clarification, the recombination of the AVV to remove its infectivity can restore virulence after attenuation. It has a probability of triggering a latent or persistent infection for some vectors. In terms of cost, it is expensive in large-scale manufacturing (Haque and Pant 2020).

1.6 Characterisation techniques for the Oxford/AstraZeneca and Janssen platform

Oxford/AstraZeneca and Janssen have summarised the experimental investigation in order to characterise the chimpanzee and serotype 26 based Adenoviral vector platforms. The Oxford/AstraZeneca structural characteristics used the orthogonal analytical methods to examine the particulate matter, molar mass, size heterogeneity, morphology, structure/identity, and biological activity. General tests were performed such as polysorbate 80 content, osmolality, pH, colour, and appearance to test the active substance. The structure/identity characterisation achieved by using viral particle and the qPCR techniques. Anion exchange high-performance liquid chromatography (AEX-HPLC) was applied in order to determine the concentration. The impurities were verified using a nuclease, Host Cell Protein, and residual DNA. The safety tests were done for endotoxin and bioburden purposes. Moreover, to determine the drug product and substance infectivity, a cell-based infectivity assay was applied (European Medicines Agency 2021b).

According to the European Medicines Agency (2021c) report, Janssen characterisation studies were conducted to investigate the structure-function relationships, biological activity, viral DNA, particle heterogeneity and capsid composition of the formulation. To highlight the biological activity, the transgene expression enzyme-linked immunosorbent assay (TGE-ELISA) was used to measure the relative level of transgene expression. Moreover, in an attempt to determine the infectivity in release testing, the quantitative PCR is based on the potency assay (QPA), which has a strong relation with the TGE-ELISA. The virus DNA characterisation technique was used to confirm the flanking regions and the transgene identity. The forced degradation studies such as the thermal stress are applied to study the structure/function relationship of the Janssen platform. The Janssen platform impurities were characterised using downstream buffer components, PER.C6 TetR host cell constituents, additives, and cell culture media components. Chromatography can be used in the purification process for impurity removal. The impurities include adenovirus proteins- post-translationally modified forms, aggregates and incomplete or empty Adenoviral particles. Janssen platform active substance specification tests contained the reversed-phase high-performance liquid chromatography (RP-HPLC) for viral identity via virus protein fingerprinting and the ID-PCR; the impurities (ELISA for the host cell protein and qPCR for the host cell DNA); in quantification purposes (VP-qPCR for the virus particle); the safety tests were done for endotoxin and bioburden purposes and general tests such as pH, polysorbate 80 concentration and appearance.

1.7 Adenoviral vector platform conclusion

To conclude, this chapter has illustrated a model of stabilised Adenoviral vector platform from the 10 platforms used for tackling the SARS-COV-2 viruses such as Oxford/AstraZeneca (ChAdOx1 nCoV-19) and Janssen (Ad26.Cov2.S). This chapter has shown 2 types of AVV platforms, the first was chimpanzee Adenoviral vector used by Oxford/AstraZeneca and the second adenovirus type 26 manufactured by Janssen. These platforms followed the same method in vaccine manufacturing, which was the replication-incompetent vector. The findings among

Oxford/AstraZeneca and Janssen platforms showed that there is a matching among their content of formulation, which are polysorbate 80 (E433), ethanol 95% and sodium chloride. However, the difference is especially for those functioning as a pH adjuster, buffering agent and stabiliser/tonicifier. Adenoviral vectors showed to have a strong humoral and cellular immunity, its application to the mucosal surface and long-term gene expression. In contrast, lack or over attenuation happen with the AVV in addition to immune response misdirection. Also, it is expensive for large-scale manufacturing. The most obvious techniques performed by Oxford/AstraZeneca and Janssen for the Adenoviral vector platform, which was orthogonal analytical methods to examine the biological activity, safety tests, particle/size heterogeneity, infectivity tests and product-related impurities.

Overall, this chapter strengthens the idea that using AVV platform is the best option especially for countries that they are suffering from a high-temperature environment and needs lower temperature refrigerators for making the vaccine more stable. As a result, the Adenoviral vector such as ChAdOx1 nCoV-19 and Ad26.Cov2.S formulations can be stored at room temperature 2-8 °C, and there is no need to be stored at lower temperatures.

CHAPTER 2

The model of un-stabilised COVID-19 vaccine: mRNA platform

2.1 INTRODUCTION

Since the isolation of mRNA in 1961, mRNA platform has been shown to induce both of cellular and humoral immune response. mRNA is a safe vector that does not interact with the genome (Meselson et al. 1961; Watson et al. 1961). On the one hand, mRNA platform is one of the promising alternative vaccines to the conventional one. In animal models, mRNA-based therapies elicit a potent immune response against infectious diseases. Each mRNA platform has an optimised sequence that is encapsulating in a lipid form. However, mRNA vaccine application has been restricted because of its instability and the inefficient of its delivery in vivo (Pardi et al. 2018). There was a need to advance a COVID-19 vaccine quickly. Therefore, all the potential platforms were investigated because of the need for it quickly. Even though in the past, mRNA platform shown to be unstable and inefficient in its delivery. It ended up being a successful candidate platform and this chapter is going to talk about the Pfizer/BioNTech and Moderna mRNA platform, as these are examples of the un-stabilised mRNA platform.

2.1.1 Introduction to Pfizer/BioNTech COVID-19 vaccine made using mRNA platform

The BNT162b2 vaccine developed by the Pfizer/BioNTech pharmaceutical companies. BNT162b2 vaccine formulated as a lipid-nucleoside modified mRNA

nanoparticle encodes a mutant called P2 mutant spike protein. It induces a blunt innate immune system, which results in increasing the antigen expression. Once the intramuscular injection made, the vaccine can transfect the optimised mRNA platform into the host cells. Through a mixing process of the dissolved LNP and the RNA, an encapsulating LNP-RNA is formed (Figure 3).

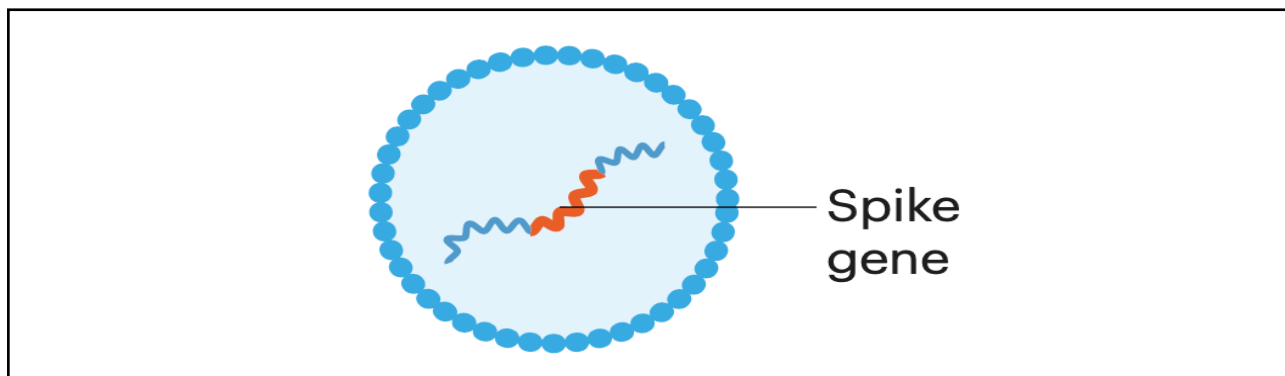


Figure (3): The lipid-nucleoside modified mRNA nanoparticle encodes a mutant called P2 mutant spike protein – copied from Krammer (2020 p.520 fig.3).

Additionally, after the intramuscular injection injected, the cells start their uptake of LNPs. Then the mRNA vaccine starts releasing its LNP contents into the cytosol that can translate the encoded spike protein. Intracellularly, mRNA platform rapidly degraded. It ends up with a spike protein-peptide presenting on the cell surface, which can trigger a T-cell immune response against the SARS-COV-2 virus spike protein (World Health Organisation 2021a).

2.1.2 Introduction to Moderna COVID-19 vaccine made using mRNA platform

The mRNA-1273 vaccine produced by the Vaccine Research Center at the National Institute of Allergy and Infectious Diseases and Moderna pharmaceutical company. The mRNA-1273 vaccine is an mRNA-encapsulated LNP that express “the SARS-COV-2 spike glycoprotein” (European Medicines Agency 2021d; World Health Organisation 2021d). The SARS-COV-2 spike protein induce a cellular and

humoral immune response. The encoded antigen spike protein includes Open Reading Frame - the 5' untranslated region (UTR) - and 3' untranslated region - polyA tail (Figure 4) (European Medicines Agency 2021d).

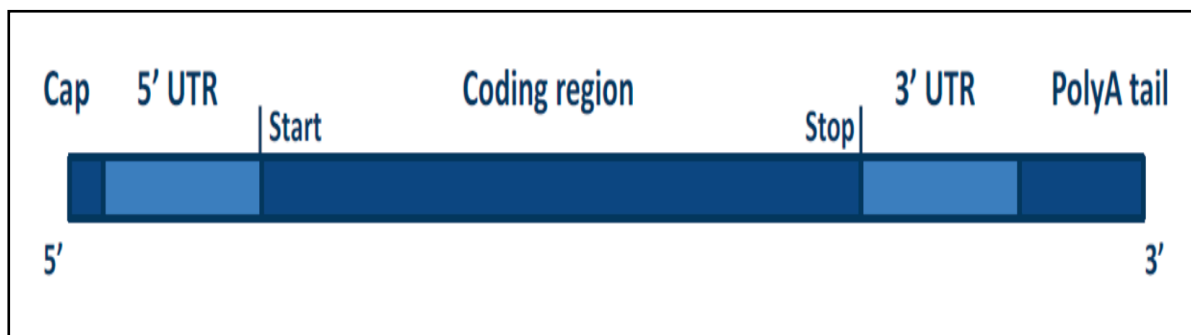


Figure (4): The structure of the encoded antigen spike protein including the 5' and 3' untranslated regions - copied from European Medicines Agency (2021d p.17 fig.1).

2.2 Pfizer/BioNTech COVID-19 vaccine

The Pfizer/BioNTech COVID-19 vaccine (BNT162b2) prevents the SARS-COV-2 virus infection through the active immunisation for those aged 16 years and older (Medicines & Healthcare products Regulatory Agency 2021b).

2.2.1 The content, storage conditions and the physical state of the formulation

This part discusses BNT162b2 vaccine content, storage conditions and the physical state of the formulation. Table 3 highlights the BNT162b2 vaccine content of the formulation, which contains mRNA particle and other excipients with their reported concentrations.

Table 3: The content of Pfizer/BioNTech COVID-19 vaccine formulation with their reported concentrations (Medicines & Healthcare products Regulatory Agency 2021b).

* The Polyethylene glycol/macrogol (PEG) is part of the ALC-0159 excipient that included in this formulation.

¹ ALC-0315: (4-hydroxybutyl) azanediyl) bis(hexane-6,1-diyl) bis (2-hexyldecanoate).

² ALC-0159: 2[(polyethylene glycol)-2000]-N,N-ditetradecylacetamide.

³ DSPC: 1,2-Distearoyl-sn-glycero-3-phosphocholine.

Pfizer/BioNTech COVID-19 vaccine (BNT162b2) formulation		
1 dose (0.3 ml)	The content of the formulation.	Concentrations per dose.
mRNA particle	BNT162b2 RNA particles.	30 µg particles (World Health Organisation 2021f).
Other excipients	1- ALC-0315 ¹	0.43 mg (World Health Organisation 2021f).
	2- ALC-0159 ^{2, *}	0.05 mg (World Health Organisation 2021f).
	3- DSPC ³	0.09 mg (World Health Organisation 2021f).
	4- Cholesterol.	0.2 mg (World Health Organisation 2021f).
	5- Potassium chloride.	0.01 mg (World Health Organisation 2021f).
	6- Potassium dihydrogen phosphate.	0.01 mg (World Health Organisation 2021f).
	7- Sodium chloride.	0.36 mg (World Health Organisation 2021f).
	8- Disodium hydrogen phosphate dihydrate.	0.07 mg (World Health Organisation 2021f).
	9- Sucrose.	6mg (World Health Organisation 2021f).
	10- Water for injections.	Not reported.

The content of Pfizer/BioNTech formulation has some different mRNA particle and other excipients from Moderna formulation such as ALC-0315 and ALC-0159, which works to provide a functional role for the lipid nanoparticle; potassium dihydrogen phosphate, sodium chloride, disodium hydrogen phosphate dihydrate and potassium chloride acting as buffer component (European Medicines Agency 2021a). In contrast to Pfizer/BioNTech formulation, however, Moderna formulation used Lipid SM-102 and PEG2000-DMG as a carrier and protectants for the mRNA platform; Tromethamol and Tromethamol hydrochloride were used as a neutralising for the buffer component.

The knowledge of BNT162b2 vaccine storage conditions and the physical state is crucial for a better understanding of mRNA stability. There is a need for BNT162b2 vaccine to be stored for up to 6 months at ultra-low freezing temperature. The BNT162b2 vaccine storage temperature is $-70\text{ }^{\circ}\text{C} \pm 10\text{ }^{\circ}\text{C}$, which needs to control the storage with a very low-temperature by using dry ice temperature-controlled thermal shippers throughout transportation processes (World Health Organisation 2021a). Also, it should not re-frozen while the vaccine thaws. During the storage process, the packaging uses to minimise the formulation from ultraviolet light and sunlight exposure. The colour of the BNT162b2 vaccine product is off-white frozen dispersion (World Health Organisation 2021f). Accordingly, it seems BNT162b2 vaccine needs some improvement for the formulation storage within the acceptable degree of temperatures, which makes it available during the shipping process without any obstacles.

2.3 Moderna COVID-19 vaccine

The Moderna COVID-19 vaccine (mRNA-1273) prevents the SARS-COV-2 virus through the “active immunisation” of those aged 18 years old and older (World Health Organisation 2021h).

2.3.1 The content, storage conditions and the physical state of the formulation

This part discusses mRNA-1273 vaccine content, storage conditions and the physical state of the formulation. Table 4 highlights the mRNA-1273 vaccine content of the formulation which contains a viral particle and other excipients with their reported concentrations.

Table 4: The content of Moderna COVID-19 vaccine formulation with their reported concentrations (Medicines & Healthcare products Regulatory Agency 2021c).

*The Polyethylene glycol/macrogol (PEG) is part of the PEG2000-DMG excipient that included in below formulation.

¹ DSPC: 1,2-distearoyl-sn-glycero-3-phosphocholine.

² PEG2000-DMG: 1,2-Dimyristoyl-rac-glycero-3-methoxypolyethylene glycol-2000.

Moderna COVID-19 vaccine (mRNA-1273) formulation		
1 dose (0.5 ml)	The content of the formulation.	Concentrations in the final product (mg/ml).
mRNA particle	mRNA-1273 particles.	0.20 (World Health Organisation 2021h).
Other excipients	1- Lipid SM-102.	2.15 (World Health Organisation 2021h).
	2- Cholesterol.	0.94 (World Health Organisation 2021h).
	3- DSPC ¹	0.55 (World Health Organisation 2021h).
	4- PEG2000-DMG ²	0.23 (World Health Organisation 2021h).
	5- Tromethamol.	0.61 (World Health Organisation 2021h).
	6- Tromethamol hydrochloride.	2.35 (World Health Organisation 2021h).
	7- Acetic acid.	0.085 (World Health Organisation 2021h).
	8- Sodium acetate trihydrate.	0.237 (World Health Organisation 2021h).
	9- Sucrose.	87 (World Health Organisation 2021h).
	10- Water for injections.	Not reported.

The content of Moderna formulation has some same mRNA particle and other excipients from Pfizer/BioNTech platform such as DSPC, cholesterol, sucrose and water for injection (World Health Organisation 2021f; World Health Organisation 2021h).

A better understanding of mRNA-1273 storage conditions and physical state is crucial for more knowledge about mRNA stability. mRNA-1273 vaccine shelf-life storage is $-20^{\circ}\text{C} \pm 5^{\circ}\text{C}$. According to the demonstrated data, when the mRNA vaccine stored at -70°C , there was no change in the biophysical state of the LNP and the mRNA purity. However, at 25°C , 5°C and -20°C , the chemical degradation of mRNA was observed. Generally, the final proposed storage for the mRNA-1273

vaccine was -20°C (European Medicines Agency 2021d). The colour of the vaccine product is white to off-white, and it is a frozen dispersion formulation (European Medicines Agency 2021d; National Pharmacy Association 2021).

2.4 The strengths of the mRNA platform

In vaccine development, each platform has strengths and weaknesses. This part intends to discuss the mRNA platform strengths. In terms of the mRNA effects on the immune system, it can induce humoral and cellular immunity against the introduced antigens. In regards to cytosolic translocation, it can enhance the direct delivery of the antigen expression into the cytosol (Haque and Pant 2020). Regarding its manufacturing process, mRNA platform produced with a rapid capacity (Haque and Pant 2020) and completely produced in vitro (Krammer 2020). In terms of its lipid moieties, mRNA platform designed for self-adjuvating purposes. Further, with its genetic expression, mRNA platform does not interact with the genome. For the causation of the adverse effects, it is less likely to cause allergens (Haque and Pant 2020) as it is readily adaptable (Crommelin et al. 2021b).

2.5 The weaknesses of the mRNA platform

mRNA platform has six key weaknesses in vaccine development. Regarding immunity, mRNA has a limitation to its immunogenicity, which encodes few fragments rather than the whole virus. The immunostimulation weaknesses happen due to the lack of endosomal RNA receptors interact with the mRNA platform. Regarding its storage, mRNA platform needs to be storing at a cooler temperature (Haque and Pant 2020). According to Krammer (2020) clarification, mRNA is a new technology and the needs for frozen storage might encounter unclear issues in the long term regarding its storage stability. In mRNA manufacturing, there are some challenges in vivo. Concerning drug delivery, as the vaccine platform administering

via injection, hence it is less likely to induce a strong mucosal immunity (Krammer 2020).

2.6 Characterisation techniques for the Pfizer/BioNTech and Moderna platform

An experimental investigation was conducted by Pfizer/BioNTech and Moderna to characterise the BNT162b2 and mRNA-1273 platforms. In terms of the BNT162b2 platform, analytical characterisation methods were used separately such as Liquid Chromatography–Ultraviolet/Mass Spectrometry (LC-UV/MS) and RP-HPLC to analyse the physico-chemical characteristics of 3' poly(A) tail and the 5' cap structure; orthogonal method, oligonucleotide mapping and Next Generation Sequencing (NGS) technology were applied to confirm the primary structure. Accordingly, the RNA sequence results were confirmed the quality attributes and the expected sequence including the full-length nucleotide sequence after using these techniques. Further specifications were performed to test the active substance colouration and clarity using the appearance test; UV spectroscopy for the RNA concentration (content); Capillary Gel Electrophoresis to characterise the RNA integrity; ddPCR to characterise the Poly(A) Tail; RT-PCR for the encoded RNA sequence identification; qPCR to look at the Residual DNA Template; Immunoblot for the dsRNA; bacterial endotoxin and bioburden (European Medicines Agency 2021a).

Regarding the mRNA-1273 platform, specification tests used to test the active substances such as RT- Sanger sequencing for the platform identification; UV spectroscopy to characterise the total RNA concentration (content); RP-HPLC for the vaccine purity, impurities and the product percentage of the poly A tailed RNA; qPCR to look at the Residual DNA Template; RP-UPLC to quantify the product percentage of the 5' Capped; bacterial endotoxin and bioburden (European Medicines Agency 2021d). The above specification tests for the BNT162b2 and mRNA-1273 platform gave acceptable results for their active substances to be authorised.

2.7 Problems of the mRNA platform including its instability

In the pharmaceutical biotechnology industry, the instability sources of mRNA-based therapies may hinder its potential work. An example of unstable mRNA platform is the Pfizer/BioNTech and Moderna vaccine (Tinari 2021). This part clarifies some sources that affect mRNA stability (Pardi et al. 2018). mRNA platform is susceptible to both chemical and enzymatic pathways of degradation (Geall et al. 2013). It is highly sensitive to degradation because of its single-stranded structure, divalent ions, and RNases of the buffer formulation (Brawerman 1974; Burgess 2012; Muralidhara et al. 2016). The other major instability source of the mRNA platform is the unstable factors in the 3' untranslated region (UTR) (Xu et al. 2020).

Accordingly, a better understanding of mRNA properties and the causes of its instability will help us select more appropriate technologies for a stabilised mRNA platform to be shipped with ambient temperatures (Crommelin et al. 2021a). mRNA platform has got several potentials as it is highly immunogenic, but its instability makes it challenging. The pharmaceutical industry is interested in identifying potential ways of stabilising the mRNA vaccine. Therefore, the next section will discuss the potential application of whether the human serum albumin could stabilise mRNA platform.

2.8 The application of the human serum albumin as a stabiliser for mRNA platform

2.8.1 Introduction

Knowledge of the human serum albumin (HSA) properties and characteristics is crucial to understand its approach in stabilising biopharmaceuticals and the mRNA platform in particular. Human serum albumin is a very stable protein and is characterised by a long half-life. Albumin is also the most abundant protein in plasma

(Sleep et al. 2013). Structurally it is a multi-domain monomeric protein with a major role in the transport of structurally diverse compounds and in maintaining the oncotic pressure among the body compartments (Fanali et al. 2012). Its structural flexibility determines its multifunctional role in the interaction with endogenous and exogenous compounds. It is interacting with the intracellular and extracellular viral components as it is highly recommended as a deliverer, therapeutic material and stabiliser for drugs (Mani Mishra et al. 2020).

2.8.2 The structure-function relationship of human serum albumin

Human serum albumin is a 585 amino acids single polypeptide chain with molecular weight of 66.5 kDa. The HSA polypeptide chain has no carbohydrate moiety with a shortage of methionine and tryptophan residues, and a high amount of charged residues including aspartic acid, arginine, lysine and glutamic acid (Theodore Peters 1995). The HSA shape in the solution is different (Nicholson et al. 2000) as it is flexible molecule and its variations depend on the binding with ligands and the environmental conditions (Peters Jr 1995). Human serum albumin is a versatile carrier protein for advancing the pharmacokinetic profile and drug targeting of protein-based drugs and peptides (Kratz 2008). According to Larsen et al. (2016), human serum albumin has multiple engagement cellular receptors and ligand binding sites, which interact with a receptor called neonatal Fc. These properties make HSA more attractive candidate macromolecules for drug delivery targeting via covalent conjugation bond attachment. As with HSA solubility, it is a water-soluble protein due to its high overall negative charge at neutral pH. Figure 5 shows the classical 3-D heart-shaped structure of the HSA obtained by using X-ray crystallography (Larsen et al. 2016).

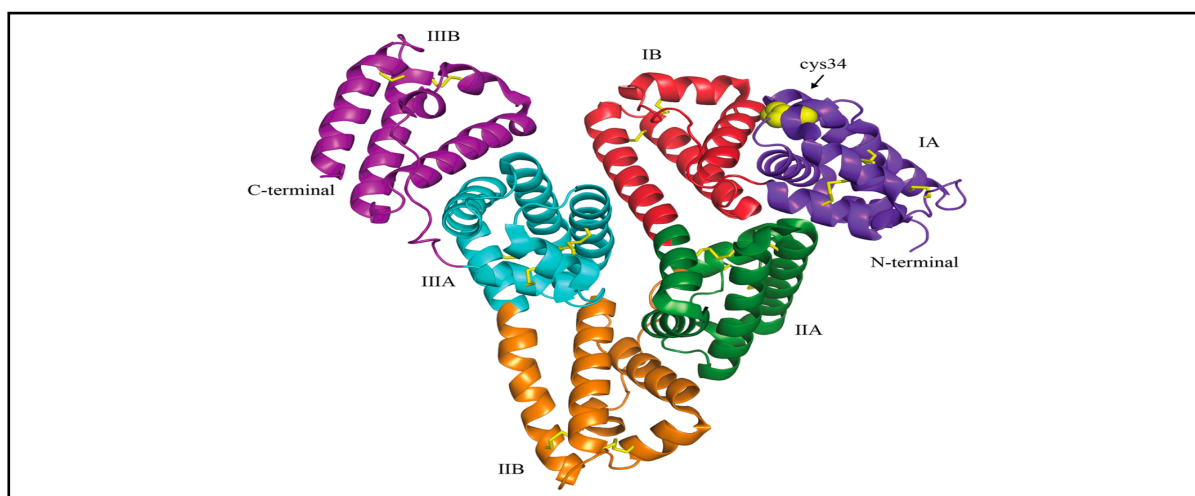


Figure 5: The tertiary crystal structure of the human serum albumin with its three domains (PDB 1e7e). Domain one (IA; purple and IB; red); domain two (IIA; green and IIB; orange) and domain three (IIIA; blue and IIIB; violet). In domain one (IA) highlights the existence of cysteine 34 residues that have disulfide bridges showing yellow sphere sticks – Copied from Larsen et al. (2016 p.2 fig.1).

Cysteine at position 34 (cys34) contributes together with the Methionines, to the anti-oxidising properties of the HSA, which contains a single free thiol group (-SH) for covalent attachment with drugs and antioxidant properties. The single free cysteine residues make HSA also attractive for drug delivery (Quinlan et al. 2005).

Accordingly, the understanding of plasma-derived human serum albumin mechanism for stabilising transfer RNA (tRNA), can be a key tool to apply in developing stable mRNA platform.

2.9 The interaction of human serum albumin for stabilising tRNA with a potential for mRNA platform

The serum-derived human albumin is a major target for nucleobases, nucleotides, RNA and DNA binding (Malonga et al. 2006a). According to Malonga et al. (2006b) paper, in aqueous solution, it was tested the interaction of HSA with the tRNA. Concerning transfer RNA, it is the physical link between mRNA that encodes

genetic information and proteins (Giegé et al. 1998). To determine the tRNA-HSA complexes, association constant, the changes in the HSA secondary structure and the mode of HSA binding; FTIR spectroscopic and Affinity capillary electrophoresis were used. The result showed 2 types of the tRNA-HSA complexes bounded. The first type, HSA main binding sites on tRNA are PO₂ backbone group and G-C bases. The second type, the HSA parts such as NH₂ groups, C–N and C=O are the main sites of binding with tRNA (Malonga et al. 2006b). Accordingly, the complex binding among tRNA-HSA showed the tRNA stabilised with no change in the conformation and the secondary structure of the HSA protein remained stable, as well (Malonga et al. 2006b).

mRNA acts as a molecule with an abundance of information between translating ribosomes and the DNA (Del Campo et al. 2015). Also, the mRNA consists of G (guanine) -C (cytosine) bases (Hames and Hooper 2011). As shown in Van Hoecke and Roose (2019) article, mRNA has a negative charge. It is obvious from the interaction of HSA with tRNA that HSA has positive charges came from NH₂ groups, C–N and C=O. Previous reviews have only focused on tRNA to address its stability with HSA instead of the mRNA. In the case of mRNA, it is possible for the HSA to stabilise mRNA platform as the same as did with the tRNA from the positive-negative interaction.

2.10 mRNA platform conclusion

To sum up, this chapter has shown a model of un-stabilised mRNA platform from the 10 platforms used for tackling the SARS-COV-2 virus such as Pfizer/BioNTech (BNT162b2) and Moderna (mRNA-1273). This chapter has illustrated the Pfizer/BioNTech and Moderna platforms, which are lipid-nucleoside modified mRNA nanoparticle encodes the SARS-COV-2 spike glycoprotein. These platforms followed the same method in vaccine manufacturing, by encapsulating the encoded mRNA platform in a lipid nanoparticle. This chapter has found that Pfizer/BioNTech and Moderna platforms showed a similarity among their content of

formulation, which are DSPC, cholesterol, sucrose, and water. On the other hand, the disparities are for those functioning as a lipid nanoparticle, buffer component, protectants, and carrier for the mRNA and for maintaining the pH at low values. mRNA illustrated to induce a strong humoral and cellular immunity, its direct delivery to the cytosol and rapid manufacturing capacity process. Also, it is designed to be self-adjuvating with less interaction with genome. In contrast, the main weakness is needs to be storing at a lower frozen temperature, which affect on the long-term storage stability.

The most obvious techniques performed by Pfizer/BioNTech and Moderna for the mRNA platform, which were RP-HPLC for the vaccine purity and to analyse the physico-chemical characteristics of 3' poly(A) tail and the 5' cap structure. Also, the UV spectroscopy were used to characterise the total RNA concentration (content). Moreover, mRNA have sources of instability, which are susceptible to both chemical and enzymatic pathways of degradation because of its single-stranded structure, divalent ions, and RNases of the buffer formulation. Additionally, it is unstable factors in the 3' untranslated region. Overall, this chapter strengthens the idea that mRNA is unstable platform and needs -70°C temperature refrigerators for making the vaccine more stable for high-temperature environment countries. As a result, this chapter suggested the potential application of the serum-derived human albumin as a stabiliser for the mRNA platform. It was shown the HSA stabilise the mRNA from the positive negative interaction among them.

CHAPTER 3

Concluding Remarks and Perspectives

Our short review has considered a model of stabilised (AVV) and un-stabilised (mRNA) platforms from 10 platforms that used for tackling SARS-COV-2 virus. Oxford/AstraZeneca and Janssen are examples on AVV platform, however, Pfizer/BioNTech and Moderna are examples on mRNA platforms. It has discussed AVV including the chimpanzee Adenoviral and adenovirus type 26 are more stabilised platforms than the mRNA nanoparticle platform. The findings showed that AVV and mRNA platforms have their own content of the formulation even for the same platform with a few similarities. Also, both of AVV and mRNA platforms illustrated to induce a strong humoral and cellular immunity. Nonetheless, mRNA was un-stabilised form and needs to be storing at a lower frozen temperature, which affect on the long-term storage stability. This due to its instability sources, which are susceptible to both chemical and enzymatic pathways of degradation; it's unstable factors in the 3' untranslated region; it's single-stranded structure, divalent ions, and RNases of the buffer formulation.

The most obvious techniques performed by Oxford/AstraZeneca and Janssen for the Adenoviral vector platform, which was orthogonal analytical methods to examine the biological activity, safety tests, particle/size heterogeneity, infectivity tests and product-related impurities. On the other hand, Pfizer/BioNTech and Moderna examined the mRNA platform through the RP-HPLC for the vaccine purity and to analyse the physico-chemical characteristics of 3' poly(A) tail and the 5' cap structure. Also, the UV spectroscopy were used to characterise the total RNA concentration (content). Overall, this research paper has strengthened the idea that the AVV is a stabilise form of Covid-19 vaccine, which can be stored at 2-8 °C and there is no need for further manipulations. However, mRNA is un-stabilised form of

Covid-19 vaccine, which can be stored at -70°C and this storage making the vaccine less stable especially for high-temperature environment countries. The potential application of the serum-derived human albumin (HSA) as a stabiliser for the mRNA platform is clearly worth exploring in more detail not just for stabilising the mRNA platform vaccines but also the Adenovirus based ones. Further research is indicated including the possible effects of non-specific interactions with antibodies generated by these vaccines. This will be the subject for the (experimental) part of this MRes project.

List of references

- ASTRAZENECA, A. 2021. *Product Information as approved by the CHMP on 29 January 2021, pending endorsement by the European Commission* [Online]. Available: https://www.ema.europa.eu/en/documents/product-information/covid-19-vaccine-astrazeneca-product-information-approved-chmp-29-january-2021-pending-endorsement_en.pdf [Accessed 1 May 2021].
- ASTUTI, I. & YSRAFIL. 2020. Severe Acute Respiratory Syndrome Coronavirus 2 (SARS-CoV-2): An overview of viral structure and host response. *Diabetes & Metabolic Syndrome: Clinical Research & Reviews*, 14(4), 407-412.
- BANERJI, A., WOLFSON, A. R., WICKNER, P. G., COGAN, A. S., MCMAHON, A. E., SAFF, R., ROBINSON, L. B., PHILLIPS, E. & BLUMENTHAL, K. G. 2021. COVID-19 Vaccination in Patients with Reported Allergic Reactions: Updated Evidence and Suggested Approach. *The Journal of Allergy and Clinical Immunology. in Practice*, 9(6), 2135-2138.
- BRAWERMAN, G. 1974. Eukaryotic messenger RNA. *Annual review of biochemistry*, 43(1), 621-642.
- BURGESS, D. J. 2012. RNA stability: Remember your driver. *Nature reviews. Genetics*, 13(2), 72-72.
- CHENG, C., WANG, L., KO, S.-Y., KONG, W.-P., SCHMIDT, S. D., GALL, J. G., COLLOCA, S., SEDER, R. A., MASCOLA, J. R. & NABEL, G. J. 2015. Combination recombinant simian or chimpanzee adenoviral vectors for vaccine development. *Vaccine*, 33(51), 7344-7351.
- CLÉNET, D. 2018. Accurate prediction of vaccine stability under real storage conditions and during temperature excursions. *European Journal of Pharmaceutics and Biopharmaceutics*, 125, 76-84.
- CROMMELIN, D. J., ANCHORDOQUY, T. J., VOLKIN, D. B., JISKOOT, W. & MASTROBATTISTA, E. 2021a. Addressing the cold reality of mRNA vaccine stability. *Journal of Pharmaceutical Sciences*, 110(3), 997-1001.
- CROMMELIN, D. J., VOLKIN, D. B., HOOGENDOORN, K. H., LUBINIECKI, A. S. & JISKOOT, W. 2021b. The science is there: key considerations for stabilizing viral vector-based Covid-19 vaccines. *Journal of pharmaceutical sciences*, 110(2), 627-634.
- DEL CAMPO, C., BARTHOLOMÄUS, A., FEDYUNIN, I. & IGNATOVA, Z. 2015. Secondary structure across the bacterial transcriptome reveals versatile roles in mRNA regulation and function. *PLoS genetics*, 11(10), e1005613-e1005613.
- EUROPEAN CENTRE FOR DISEASE PREVENTION AND CONTROL. 2021. Coronaviruses. *European Centre for Disease Prevention and Control*.
- EUROPEAN MEDICINES AGENCY. 2021a. *COVID-19 mRNA vaccine (nucleoside-modified)* [Online]. Committee for Medicinal Products for Human Use (CHMP). Available: https://www.ema.europa.eu/en/documents/assessment-report/comirnaty-epar-public-assessment-report_en.pdf [Accessed 1 April 2021].
- EUROPEAN MEDICINES AGENCY. 2021b. *COVID-19 Vaccine AstraZeneca* [Online]. Committee for Medicinal Products for Human Use (CHMP). Available: https://www.ema.europa.eu/en/documents/assessment-report/vaxzevria-previously-covid-19-vaccine-astrazeneca-epar-public-assessment-report_en.pdf [Accessed 20 March 2021].

- EUROPEAN MEDICINES AGENCY. 2021c. *COVID-19 Vaccine Janssen* [Online]. Committee for Medicinal Products for Human Use (CHMP). Available: https://www.ema.europa.eu/en/documents/assessment-report/covid-19-vaccine-janssen-epar-public-assessment-report_en.pdf [Accessed 1 April 2021].
- EUROPEAN MEDICINES AGENCY. 2021d. *COVID-19 Vaccine Moderna* [Online]. Committee for Medicinal Products for Human Use (CHMP). Available: https://www.ema.europa.eu/en/documents/assessment-report/covid-19-vaccine-moderna-epar-public-assessment-report_en.pdf [Accessed 4 April 2021].
- FANALI, G., DI MASI, A., TREZZA, V., MARINO, M., FASANO, M. & ASCENZI, P. 2012. Human serum albumin: from bench to bedside. *Molecular aspects of medicine*, 33(3), 209-290.
- GEALL, A. J., MANDL, C. W. & ULMER, J. B. RNA: the new revolution in nucleic acid vaccines. *Seminars in immunology*, 2013. Elsevier, 152-159.
- GIEGÉ, R., SISSLER, M. & FLORENTZ, C. 1998. Universal rules and idiosyncratic features in tRNA identity. *Nucleic acids research*, 26(22), 5017-5035.
- GUO, J., MONDAL, M. & ZHOU, D. 2018. Development of novel vaccine vectors: Chimpanzee adenoviral vectors. *Human vaccines & immunotherapeutics*, 14(7), 1679-1685.
- GUO, Y.-R., CAO, Q.-D., HONG, Z.-S., TAN, Y.-Y., CHEN, S.-D., JIN, H.-J., TAN, K.-S., WANG, D.-Y. & YAN, Y. 2020. The origin, transmission and clinical therapies on coronavirus disease 2019 (COVID-19) outbreak—an update on the status. *Military Medical Research*, 7(1), 11-11.
- HAMES, D. & HOOPER, N. 2011. *BIOS Instant Notes in Biochemistry*, London, Taylor & Francis Group.
- HAQUE, A. & PANT, A. B. 2020. Efforts at COVID-19 Vaccine Development: Challenges and Successes. *Vaccines*, 8(4), 739.
- HUANG, C., WANG, Y., LI, X., REN, L., ZHAO, J., HU, Y., ZHANG, L., FAN, G., XU, J., GU, X., CHENG, Z., YU, T., XIA, J., WEI, Y., WU, W., XIE, X., YIN, W., LI, H., LIU, M., XIAO, Y., GAO, H., GUO, L., XIE, J., WANG, G., JIANG, R., GAO, Z., JIN, Q., WANG, J. & CAO, B. 2020. Clinical features of patients infected with 2019 novel coronavirus in Wuhan, China. *The lancet*, 395(10223), 497-506.
- JANSSEN PHARMACEUTICAL COMPANIES. 2021. *FACT SHEET FOR HEALTHCARE PROVIDERS ADMINISTERING VACCINE (VACCINATION PROVIDERS)* [Online]. Available: <https://www.fda.gov/media/146304/download> [Accessed 25 April 2021].
- KAHN, J. S. & MCINTOSH, K. 2005. History and recent advances in coronavirus discovery. *The Pediatric infectious disease journal*, 24(11), S223-S227.
- KHARE, R., CHEN, C. Y., WEAVER, E. A. & BARRY, M. A. 2011. Advances and future challenges in adenoviral vector pharmacology and targeting. *Current gene therapy*, 11(4), 241-258.
- KRAMMER, F. 2020. SARS-CoV-2 vaccines in development. *Nature*, 586(7830), 516-527.
- KRATZ, F. 2008. Albumin as a drug carrier: design of prodrugs, drug conjugates and nanoparticles. *Journal of controlled release*, 132(3), 171-183.
- LARSEN, M. T., KUHLMANN, M., HVAM, M. L. & HOWARD, K. A. 2016. Albumin-based drug delivery: harnessing nature to cure disease. *Molecular and cellular therapies*, 4(1), 1-12.
- MALONGA, H., NEAULT, J., ARAKAWA, H. & TAJMIR-RIABI, H. 2006a. DNA interaction with human serum albumin studied by affinity capillary electrophoresis and FTIR spectroscopy. *DNA and cell biology*, 25(1), 63-68.

- MALONGA, H., NEAULT, J.-F. & TAJMIR-RIABI, H.-A. 2006b. Transfer RNA binding to human serum albumin: A model for protein–RNA interaction. *DNA and cell biology*, 25(7), 393-398.
- MANI MISHRA, P., UVERSKY, V. N. & NANDI, C. K. 2020. Serum albumin-mediated strategy for the effective targeting of SARS-CoV-2. *Medical hypotheses*, 140, 109790-109790.
- MEDICINES & HEALTHCARE PRODUCTS REGULATORY AGENCY. 2021a. *Information for UK recipients on COVID-19 Vaccine AstraZeneca (Regulation 174)* [Online]. GOV.UK. Available: <https://www.gov.uk/government/publications/regulatory-approval-of-covid-19-vaccine-astrazeneca/information-for-uk-recipients-on-covid-19-vaccine-astrazeneca> [Accessed 29 June 2021].
- MEDICINES & HEALTHCARE PRODUCTS REGULATORY AGENCY. 2021b. *Information for UK recipients on Pfizer/BioNTech COVID-19 vaccine* [Online]. GOV.UK. Available: <https://www.gov.uk/government/publications/regulatory-approval-of-pfizer-biontech-vaccine-for-covid-19/information-for-uk-recipients-on-pfizerbiontech-covid-19-vaccine> [Accessed 29 June 2021].
- MEDICINES & HEALTHCARE PRODUCTS REGULATORY AGENCY. 2021c. *Summary of Product Characteristics for COVID-19 Vaccine Moderna* [Online]. GOV.UK. Available: <https://www.gov.uk/government/publications/regulatory-approval-of-covid-19-vaccine-moderna/information-for-healthcare-professionals-on-covid-19-vaccine-moderna> [Accessed 29 June 2021].
- MEDICINES & HEALTHCARE PRODUCTS REGULATORY AGENCY. 2021d. *Summary of the Public Assessment Report for COVID-19 Vaccine AstraZeneca* [Online]. GOV.UK. Available: <https://www.gov.uk/government/publications/regulatory-approval-of-covid-19-vaccine-astrazeneca/summary-of-the-public-assessment-report-for-astrazeneca-covid-19-vaccine> [Accessed 28 June 2021].
- MESELSON, M., JACOB, F. & BRENNER, S. 1961. An unstable intermediate carrying information from genes to ribosomes for protein synthesis. *Nature*, 190(4776), 576-581.
- MURALIDHARA, B. K., BAID, R., BISHOP, S. M., HUANG, M., WANG, W. & NEMA, S. 2016. Critical considerations for developing nucleic acid macromolecule based drug products. *Drug discovery today*, 21(3), 430-444.
- NATIONAL PHARMACY ASSOCIATION. 2021. *COVID-19: Pfizer/BioNTech, Oxford/AstraZeneca and Moderna vaccines characteristics comparison chart* [Online]. Available: <http://psnc.org.uk/tees-lpc/wp-content/uploads/sites/11/2021/01/COVID-19-vaccine-characteristic-comparison-chart-14.01.21-final-1.pdf> [Accessed 29 June 2021].
- NICHOLSON, J., WOLMARANS, M. & PARK, G. 2000. The role of albumin in critical illness. *British journal of anaesthesia*, 85(4), 599-610.
- PARDI, N., HOGAN, M. J., PORTER, F. W. & WEISSMAN, D. 2018. mRNA vaccines—a new era in vaccinology. *Nature reviews*, 17(4), 261-279.
- PARK, C.-Y., KIM, K., HELBLE, M. & ROTH, S. 2021. Getting Ready for the COVID-19 Vaccine Rollout.
- PETERS JR, T. 1995. *All about albumin: biochemistry, genetics, and medical applications*, Academic press.
- PINSCHEWER, D. D. 2017. Virally vectored vaccine delivery: medical needs, mechanisms, advantages and challenges. *Swiss medical weekly*, 147(3132), w14465-w14465.

- QAMAR, M., ALQAHTANI, S., ALAMRI, M. & CHEN, L. 2020. Structural basis of SARS-CoV-2 3CLpro and anti-COVID-19 drug discovery from medicinal PLANTS.
- QUINLAN, G. J., MARTIN, G. S. & EVANS, T. W. 2005. Albumin: biochemical properties and therapeutic potential. *Hepatology*, 41(6), 1211-1219.
- RERKS-NGARM, S., PITISUTTITHUM, P., NITAYAPHAN, S., KAEWKUNGWAL, J., CHIU, J., PARIS, R., PREMSRI, N., NAMWAT, C., DE SOUZA, M., ADAMS, E., BENENSON, M., GURUNATHAN, S., TARTAGLIA, J., MCNEIL, J. G., FRANCIS, D. P., STABLEIN, D., BIRX, D. L., CHUNSUTTIWAT, S., KHAMBOONRUANG, C., THONGCHAROEN, P., ROBB, M. L., MICHAEL, N. L., KUNASOL, P. & KIM, J. H. 2009. Vaccination with ALVAC and AIDSVAX to prevent HIV-1 infection in Thailand. *New England Journal of Medicine*, 361(23), 2209-2220.
- ROWE, W. P., HUEBNER, R. J., GILMORE, L. K., PARROTT, R. H. & WARD, T. G. 1953. Isolation of a cytopathogenic agent from human adenoids undergoing spontaneous degeneration in tissue culture. *Proceedings of the Society for Experimental Biology and Medicine*, 84(3), 570-573.
- SINGH, S., KUMAR, R. & AGRAWAL, B. 2019. Adenoviral vector-based vaccines and gene therapies: Current status and future prospects. *Adenoviruses*(Chapter 4), 53-91.
- SLEEP, D., CAMERON, J. & EVANS, L. R. 2013. Albumin as a versatile platform for drug half-life extension. *Biochimica et Biophysica Acta (BBA)-General Subjects*, 1830(12), 5526-5534.
- STANBERRY, L. R. & STRUGNELL, R. 2011. Vaccines of the future. *Perspectives in Vaccinology*, 1(1), 151-199.
- TATSIS, N. & ERTL, H. C. 2004. Adenoviruses as vaccine vectors. *Molecular Therapy*, 10(4), 616-629.
- THEODORE PETERS, J. R. 1995. *All about albumin: biochemistry, genetics, and medical applications*, Elsevier Science.
- TIAN, X., LI, C., HUANG, A., XIA, S., LU, S., SHI, Z., LU, L., JIANG, S., YANG, Z., WU, Y. & YING, T. 2020. Potent binding of 2019 novel coronavirus spike protein by a SARS coronavirus-specific human monoclonal antibody. *Emerging microbes & infections*, 9(1), 382-385.
- TINARI, S. 2021. The EMA covid-19 data leak, and what it tells us about mRNA instability. *bmj*, 372, n627-n627.
- TURNER, P. J., ANSOTEGUI, I. J., CAMPBELL, D. E., CARDONA, V., EBISAWA, M., EL-GAMAL, Y., FINEMAN, S., GELLER, M., GONZALEZ-ESTRADA, A., GREENBERGER, P. A., LEUNG, A. S. Y., LEVIN, M. E., MURARO, A., SÁNCHEZ BORGES, M., SENNA, G., TANNO, L. K., THONG, B. Y.-H. & WORM, M. 2021. COVID-19 vaccine-associated anaphylaxis: a statement of the World Allergy Organization Anaphylaxis Committee. *The World Allergy Organization Journal*, 14(2), 100517-100517.
- VAN HOECKE, L. & ROOSE, K. 2019. How mRNA therapeutics are entering the monoclonal antibody field. *Journal of translational medicine*, 17(1), 54-54.
- WATSON, J. D., GILBERT, W., GROS, F., KURLAND, C. G., RISEBROUGH, R. & HIATT, H. 1961. Unstable ribonucleic acid revealed by pulse labelling of Escherichia coli. *Nature*, 190(4776), 581-585.
- WORLD HEALTH ORGANISATION. 2021a. *Background document on mRNA vaccine BNT162b2 (Pfizer-BioNTech) against COVID-19* [Online]. World Health Organisation. Available: [https://www.who.int/publications/i/item/background-document-on-mrna-vaccine-bnt162b2-\(pfizer-biontech\)-against-covid-19](https://www.who.int/publications/i/item/background-document-on-mrna-vaccine-bnt162b2-(pfizer-biontech)-against-covid-19) [Accessed 7 March 2021].

- WORLD HEALTH ORGANISATION. 2021b. *Background document on the Janssen Ad26.COV2.S (COVID-19) vaccine: Background document to the WHO Interim recommendations for use of Ad26.COV2.S (COVID-19) vaccine* [Online]. World Health Organisation Available: <https://www.who.int/publications/i/item/WHO-2019-nCoV-vaccines-SAGE-recommendation-Ad26.COV2.S-background-2021.1> [Accessed 6 March 2021].
- WORLD HEALTH ORGANISATION. 2021c. *Background document on the Janssen Ad26.COV2.S (COVID-19) vaccine: Background document to the WHO Interim recommendations for use of Ad26.COV2.S (COVID-19) vaccine* [Online]. Available: <https://www.who.int/publications/i/item/WHO-2019-nCoV-vaccines-SAGE-recommendation-Ad26.COV2.S-background-2021.1> [Accessed].
- WORLD HEALTH ORGANISATION. 2021d. *Background document on the mRNA-1273 vaccine (Moderna) against COVID-19* [Online]. World Health Organisation. Available: [https://www.who.int/publications/i/item/background-document-on-the-mrna-1273-vaccine-\(moderna\)-against-covid-19](https://www.who.int/publications/i/item/background-document-on-the-mrna-1273-vaccine-(moderna)-against-covid-19) [Accessed 8 March 2021].
- WORLD HEALTH ORGANISATION. 2021e. *COVID-19 vaccine tracker and landscape* [Online]. World Health Organisation Available: <https://www.who.int/publications/m/item/draft-landscape-of-covid-19-candidate-vaccines> [Accessed 5 March 2021].
- WORLD HEALTH ORGANISATION. 2021f. *RECOMMENDATION FOR AN EMERGENCY USE LISTING OF COVID-19 mRNA VACCINE (NUCLEOSIDE MODIFIED) SUBMITTED BY Pfizer Europe MA EEIG* [Online]. World Health Organisation Available: https://extranet.who.int/pqweb/sites/default/files/documents/TAG-EUL_PublicReport_Pfizer_31DEC20.pdf [Accessed 9 March 2021].
- WORLD HEALTH ORGANISATION. 2021g. *Vaccine management and logistics support* [Online]. World Health Organisation Available: <https://www.who.int/teams/immunization-vaccines-and-biologicals/essential-programme-on-immunization/supply-chain/vaccine-management-and-logistics-support/> [Accessed 6 March 2021].
- WORLD HEALTH ORGANISATION. 2021h. *WHO recommendation Moderna COVID-19 mRNA Vaccine (nucleoside modified)* [Online]. World Health Organisation Available: <https://extranet.who.int/pqweb/vaccines/covid-19-mrna-vaccine-nucleoside-modified> [Accessed 10 March 2021].
- XU, S., YANG, K., LI, R. & ZHANG, L. 2020. mRNA vaccine era—mechanisms, drug platform and clinical prospection. *International Journal of Molecular Sciences*, 21(18), 1-35.



**University of
Nottingham**

UK | CHINA | MALAYSIA

Characterisation of IgG A33 hFab' and human serum albumin using hydrodynamic methods

A research paper/ review article submitted to The University of Nottingham in partial fulfilment of the requirements for the degree of Master of Research in Industrial Physical Biochemistry

MRes Industrial Physical Biochemistry

Khalil Mustafa Khalil Abu Hammad

Supervised by Professor Stephen E. Harding

Contributors: Judith Wayte, Vlad Dinu, Jacob Patten, Pallab Borah and Thomas MacCalman

**University of Nottingham
National Centre for Macromolecular Hydrodynamics
School of Biosciences, Sutton Bonington
Loughborough, Leicestershire
LE12 5RD, United Kingdom
September 2021**

Word count: 3914 words

LIST OF CONTENTS

Acknowledgements	I
Abstract	II
Abbreviations	III
1. Introduction.....	1
2. Materials and methods.....	4
2.1 Materials	4
2.2 Methods.....	4
2.2.1 Dialysis	4
2.2.2 UV spectrophotometer	5
2.2.3 Dynamic Light Scattering.....	5
2.2.4 Sodium Dodecyl Sulphate – Polyacrylamide Gel Electrophoresis.....	6
2.2.5 Analytical Ultracentrifugation- Sedimentation Equilibrium analysis.....	7
2.2.6 Analytical Ultracentrifugation- Sedimentation Velocity analysis.....	7
2.2.7 Ostwald (U-tube) capillary viscometer	8
3. Results and Discussion.....	10
3.1 Producing a pure sample of IgG A33 hFab' and HSA through dialysis and with their concentration measurements.....	10
3.2 Homogeneity/heterogeneity evaluation with dynamic light scattering	11
3.3 Molecular weight measurements.....	13
3.3.1 Sodium Dodecyl Sulphate – Polyacrylamide Gel Electrophoresis.....	13
3.3.2 Analytical Ultracentrifugation – Sedimentation Equilibrium.....	15
3.4 The assessment of purity and the presence of dimers and aggregates.....	17
3.5 Investigating a possibility of HSA and IgG A33 hFab' interactions.....	21
3.6 The analysis of the viscosity	23
4. Conclusion and Future Work.....	26
List of references.....	27
Appendix: Investigation of the effect of a non-aqueous solvent (isopropyl alcohol) on the properties of IgG A33 hFab'.....	29

Acknowledgements

The laboratory-based work part was performed in The National Centre for Macromolecular Hydrodynamics (NCMH) at the University of Nottingham. I want to thank my supervisor Dr Stephen E. Harding for his guidance and support during all the experimental work processes.

Special thanks to my academic consultant Dr Judith Wayte for her constructive comments, suggestions, and feedback. I gratefully acknowledge the technical assistance provided during the lab work by Dr Vlad Dinu, Dr Jacob Pattem, Dr Pallab Borah and Thomas MacCalman. Thanks are also to UCB Celltech biotechnology company for providing IgG A33 hFab' sample and Albumedix biotechnology company for supplying human serum albumin sample, which was used in our hydrodynamic characterisation techniques.

Abstract

Background: Hydrodynamic methods such as analytical ultracentrifugation, dynamic light scattering, SDS-PAGE, viscosity analysis, dialysis tubing and UV spectroscopy were employed. These methods were to investigate the heterogeneity/homogeneity, molecular weights, purity, the concentration measurements, solution conformations and intrinsic viscosity of IgG A 33 hFab' and human serum albumin (HSA). Both macromolecules relevant in cancer and biopharmaceutical therapies. We also investigate the properties of mixtures of the two, probing for a possible interaction, which will help in developing formulations of cancer and biopharmaceutical therapeutics in the future.

Methods: The dialysis experiment was performed to produce pure samples of HSA and IgG A33hFab' macromolecules and measuring the concentration via UV spectroscopy. Determination of the molecular weight was applied by using SDS-PAGE and sedimentation equilibrium (SE) for both macromolecules. To analyse the HSA and IgG A33 hFab' purity and the presence of possible dimers and aggregates, the SV method was performed. Also, the SV was utilised to obtain more information about the possible interaction between the IgG A33 hFab' and human serum albumin. The dynamic light scattering method was utilised to further evaluate the heterogeneity of the IgG A33 hFab' macromolecule. Viscosity measurements were applied to determine IgG A33 hFab' and human serum albumin macromolecules shape with their intrinsic viscosities, using Ostwald (U-tube) capillary viscometer.

Results: DLS results reinforced by sedimentation velocity (single peak) showed that IgG A33 hFab' is homogenous and free of aggregated particles. Its molecular weight is ~ 48- 50 kDa and monomeric state using the SDS-PAGE and SE methods. HSA molecular weight is also shown to be homogenous from sedimentation velocity with a molecular weight of 70.6 kDa using the absorbance optical system in SE method. A single sedimentation peak was also seen in mixtures of HSA with IgG A33 hFab'. This could either be due to an interaction or due to the Johnston-Ogston effect. Using ELLIPS (molecular shape) both IgG A33 hFab' and HSA are globular with very similar axial ratios. These results will advance the knowledge in biotherapeutics for an effective formulation in manufacturing process.

Keywords: Human serum albumin, IgG A33 hFab', cancer immunotherapy and macromolecules hydrodynamics.

Abbreviations

°C	Celsius
DLS	Dynamic light scattering
$D_{20,w}$	The diffusion coefficients corrected for the viscosity and density at 20.0 °C (Unit: $\text{cm}^2.\text{s}^{-1}$).
HSA	Human serum albumin
IgG A33 hFab'	Antibody fragment of the murine monoclonal antibody (MAb)
kDa	KiloDalton
M.wt	Molecular weight (kDa or g.mol^{-1})
M_w	Weight average molecular weight
$M_{w,app}$	Apparent weight average molecular weight
η_r	Relative viscosity
$[\eta]$	Intrinsic viscosity (ml/g)
η_{red}	Reduced viscosity
PBS	Phosphate – buffered saline
SV	Sedimentation velocity
SE	Sedimentation equilibrium
SDS-PAGE	Sodium Dodecyl Sulphate – Polyacrylamide Gel Electrophoresis
$s_{20,w}$	Sedimentation coefficient normalised to standard solvent conditions: density and the viscosity of water at 20.0°C. (Unit: S)
UV-spectrophotometer	Ultraviolet spectrophotometer
μl	Microliter

1. Introduction

A humanised antibody recognised by murine monoclonal antibody (MAb) fab fragment, is attracting interest due to its application in cancer immunotherapies. Its potential application is using for the treatment or diagnosis of colorectal metastases and tumours with patients in the Western world. The humanisation techniques of the chimeric antibodies showed a lower immune response -immunogenicity- in comparison with the murine monoclonal antibody (King et al. 2001). However, in cancer therapies, generally, the half-life of the fab fragment ≈ 28 min, through its conjugation with tumours due to the lower molecular weight (size) (Xenaki et al. 2017). This limitation may arise with the IgG A33 hFab' macromolecule, which ends up with a reduction of the IgG A33 hFab' macromolecule usefulness and efficacy as a therapeutic agent. Figure 1-A showing the full antibody predicted with the small size of IgG A33 hFab' fragment in Figure 1-B.

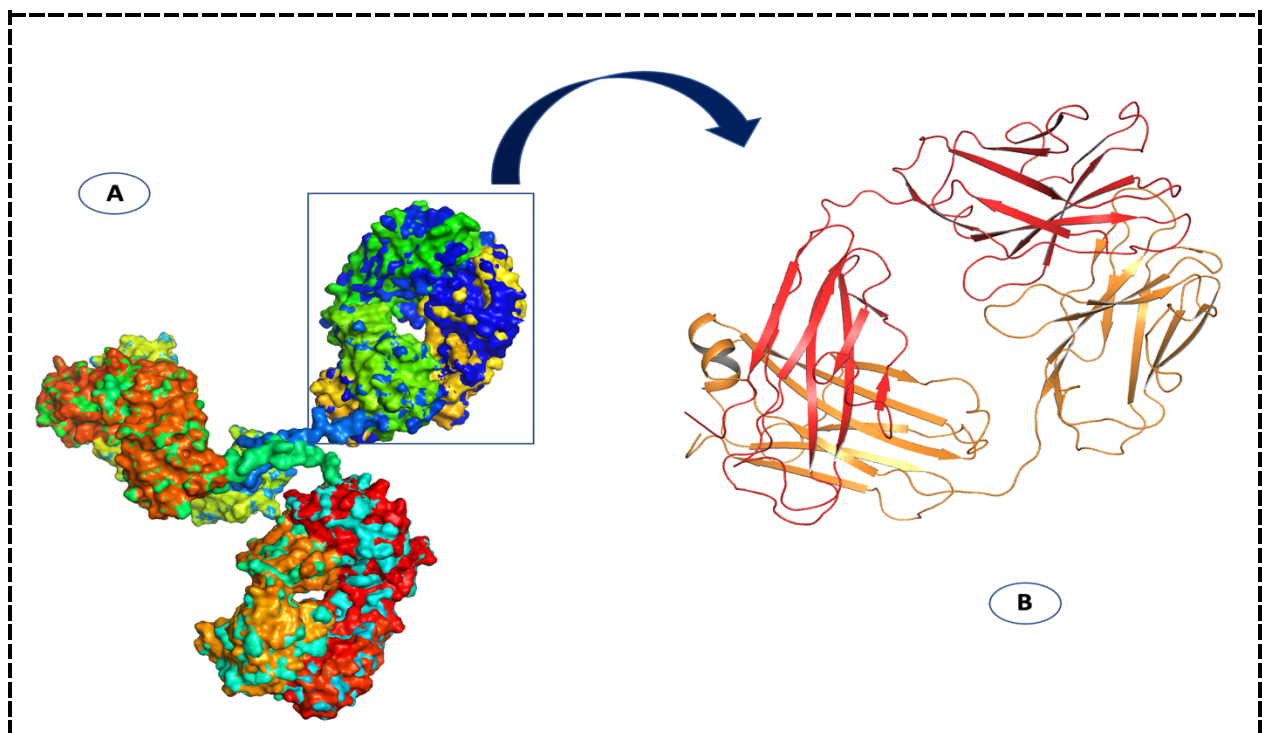


Figure 1: A surface shape of (A) full IgG2_{a/k} antibody prediction (PDBid:1IGT) and (B) is a cartoon shape of the IgG A33 hFab' macromolecule fragment. The full

IgG2_{a/k} antibody with its fab fragment created using “The Pymol Molecular Graphics System, Version 2.5.0 Schrödinger, LLC”.

The extension of biotherapeutics half-life plays a major role in improving patient's life by reducing the burdens on them. Also, the extension of half-life recognised by the biopharmaceutical industries with around 15% of the biotherapeutics was amended for this purpose (Walsh 2014). To overcome the half-life issue of the fab fragment in general and the IgG A33 hFab' particularly, however, human serum albumin (HSA) has \approx 19-21 days half-life in the human blood (see figure 2) (Sand et al. 2015). Further, HSA minimising the drug-induced cytotoxicity, enhancing the tumour specificity and maintains the active agent of therapeutics concentration such as genes, proteins, peptides, and drugs for a long period (Zeeshan et al. 2021).

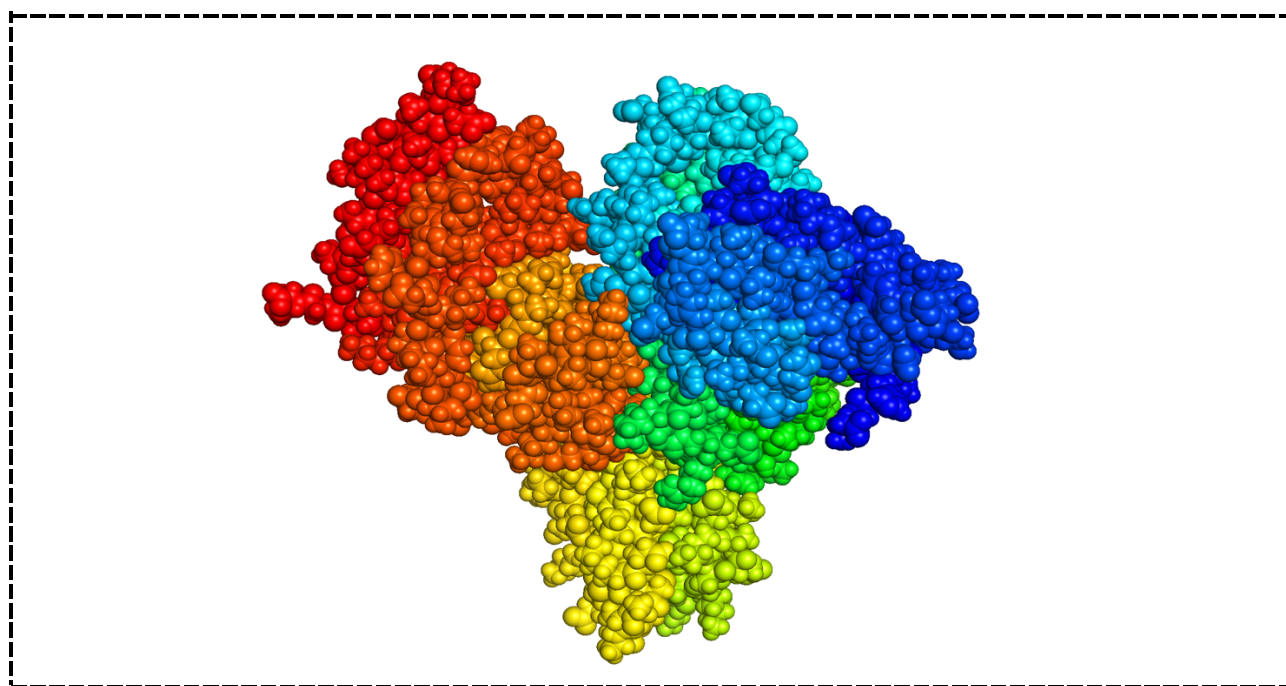


Figure 2: A tertiary structure of human serum albumin, represented as spheres in shape (PDBid: 4LB2). The HSA structure was created using “The Pymol Molecular Graphics System, Version 2.5.0 Schrödinger, LLC”.

Since the shortage of IgG A33 hFab' macromolecule half-life is the main concern in the biotherapeutics manufacturing development. The HSA can be applied to extend the IgG A33 hFab' half-life, as it is not yet known whether HSA can interact with IgG A33 hFab'. Additionally, the interaction among them will indicate if the IgG A33 hFab'

half-life can be extended or not. This experimental study aims to characterise the solution behaviour of IgG A33 hFab' and human serum albumin macromolecules using several hydrodynamic techniques, and to investigate a possible interaction between them. The objectives of this experimental study are to, first, produce pure samples of human serum albumin and IgG A33 hFab' macromolecules using a dialysis-tubing experiment, with concentration subsequently measured by UV spectrophotometer. Second, to determine the molecular weight of the IgG A33 hFab' using SDS-PAGE and sedimentation equilibrium (SE) for both macromolecules. Third, to assess the IgG A33 hFab' and the human serum albumin macromolecules purity and the presence of possible dimers and aggregates using sedimentation velocity (SV) of the analytical ultracentrifugation. This is because the interaction medium needs a pure sample of both HSA and IgG A33 hFab' and free of the aggregated particles. Additionally, to investigate a possible interaction among the IgG A33 hFab' and human serum albumin through SV, as well. Then, to further evaluate the heterogeneity of the IgG A33 hFab' by applying the dynamic light scattering method. Finally, viscosity measurements will apply to evaluate the molecular shape in solution of IgG A33 hFab' and human serum albumin macromolecules with their intrinsic viscosities, for expanding the knowledge of asymmetry/axial ratio for both of them.

2. Materials and methods

2.1. Materials

Stock solutions were prepared of IgG A33 hFab' (tWB E-017578, UCB Celltech, United Kingdom) and human serum albumin (Albumedix, United Kingdom), pH 7.0, in phosphate-buffered saline (PBS: NaCl, KH₂PO₄ and Na₂HPO₄·12H₂O), with an adjusted ionic strength (I) equal to 0.1 M. The PBS buffer was used as an aqueous solvent and stored at 2–8 °C. The 2x Laemmli sample buffer was obtained from BIO-RAD Laboratories (USA). Precision Plus Protein™ Standards, Dual colour Standards from BIO-RAD (USA) as a ladder for determining the molecular weight through the gel. The 10x Tris/Glycine/SDS buffer from BIO-RAD (USA). 2-Mercaptoethanol (≥ 99.0%, M6250, Lot # STBJ9454) was provided by Sigma-Aldrich® (USA). InstantBlue® Coomassie Protein Stain (ISB1L) lot GR3392748-1. BioDesignDialysis Tubing™ (D004) was supplied by THERMOFISHER SCIENTIFIC, BioDesign Inc. (New York, USA). Disposable cuvettes were from PLASTIBRAND® (Germany). Polystyrol/Polystyrene cuvettes with 10 × 10 × 45 mm (REF.67.74. 1) were from SARSTEDT AG& Co. (Germany). The GraphPad Prism software program was used to create plots in the Results and Discussion sections of this report.

2.2. Methods

2.2.1 Dialysis

This procedure used BioDesignDialysis Tubing™ (D004), which had 21.3 mm wet diameter and 3.57 ml/cm volume (14000 MWCO). The endings were tied tightly to avoid any leakage from inside or outside the tubing dialysis with the PBS buffer solution. The IgG A33 hFab' and HSA macromolecules were pipetted and dialysed against the PBS buffer in separate experiments for both of them. Afterwards, it was tied again from the other end, leaving a small air bubble inside the tubing bag. Later, the BioDesignDialysis Tubing™ was stored in the refrigerator at 4 °C and then the final dialysed concentration measured. This procedure was followed for both the IgG A33 hFab' and HSA samples.

2.2.2 UV spectrophotometer

The concentration measurement procedure was performed to verify the dialysed samples of IgG A33 hFab' and HSA macromolecules using a UV spectrophotometer. They were prepared and diluted in a PBS buffer in a ratio of 1:5 and 1:2, respectively. Then, the UNICAM Helios β instrument and 2 disposable cuvettes – 1 cm in length – were employed to measure these samples with PBS buffer as a reference. Five measurements were run individually for obtaining the absorbance with a fixed wavelength at $\epsilon_{280} = 1370 \text{ ml.g}^{-1}.\text{cm}^{-1}$ (IgG A33 hFab') and $538 \text{ ml.g}^{-1}.\text{cm}^{-1}$ (HSA). Afterwards, the c (mg/ml) was calculated using the Beer-Lambert Law equation as follow:

$$A = \epsilon_{280} \times b \times c \quad (1)$$

where A is the absorbance of the IgG A33 hFab' and HSA macromolecules at 280 and b is the path length of the cuvette in cm (Swinehart 1962).

2.2.3 Dynamic Light Scattering

Dynamic light scattering (DLS) measurements were done using a Malvern (ZETASIZER) Nano Series - Nano- ZS instrument. 1.0 mg/ml and 0.5 mg/ml solutions of the IgG A33 hFab' macromolecule were placed in DTS0012 - Disposable polystyrol/polystyrene sizing cuvettes (Malvern Instruments Ltd., UK). The IgG A33 hFab' sample was examined at $(20.0 \pm 0.1) ^\circ\text{C}$ through using dual angles which were 173° (Backscatter) and 13° (Forwardscatter) for the different concentrations, collected for 1 run of 120 seconds period per concertation. After that, the IgG A33 hFab' sample and the PBS buffer were filtrated from probable dust particles, airborne and large aggregates. Therefore, the sensitivity of the DLS method was considered by handling dust removal, to remove any dust particles and airborne for the light scattering detector chamber, Eppendorf tubes and the cuvettes. We used Malvern's Zetasizer commercially available software to measure the hydrodynamic sizes (r_H) in nm or μm of the IgG A33 hFab' macromolecule and the size distribution (expressed as volume fraction or %).

The translational hydrodynamic or “Stokes” radius was evaluated by the software from the translational diffusion coefficient $D_{20,w}$ calculated using Stokes equation as shown below (see, for example, Harding (1994)):

$$r_H = \frac{k_B \times T}{6 \times \pi \times \eta_{20,w} \times D_{20,w}} \quad (2)$$

where, k_B is the Boltzmann constant which is equal ($1.38062 \times 10^{-16} \frac{\text{erg}}{\text{K}}$), T is the absolute temperature in Kelvin and $\eta_{20,w}$ is the water viscosity at 20.0 °C.

2.2.4 Sodium Dodecyl Sulphate – Polyacrylamide Gel Electrophoresis

A 1 mg/ml aliquot was prepared from the IgG A33 hFab' stock solution to estimate its molecular weight using Sodium Dodecyl Sulphate – Polyacrylamide Gel Electrophoresis (SDS-PAGE). Briefly, this method followed using Mini-PROTEAN® TGX™ Precast Gels were supplied from BIO-RAD (USA). The comb and tape (green) were removed to make it ready for running by Mini-PROTEAN® Tetra Vertical Electrophoresis Cell from BIO-RAD (USA). Heating was applied for IgG A33 hFab' sample for around 5 min at ≈ 100 °C. Afterwards, 2x Laemmli sample buffer (purple) was prepared with 2-mercaptoethanol for a total volume= 100 μ l. Then, 10x Tris/Glycine/SDS buffer poured inside and outside the chambers in Mini-PROTEAN® Tetra Vertical Electrophoresis Cell, with a 9:1 concentration ratio of the RO/milli-Q water sample, which used as a running buffer, as well. It was assured that the wells are rinsed with Tris/Glycine/SDS buffer before start running the gel. The prepared samples with their gradient concentrations were loaded in wells starting with 4 μ l of the Dual colour Standards. Through running Precast Gels, the voltage was set at 80 volts for 15 min, later, it was increased to 180 volts. At the end, the cassette gel was opened and immersed in InstantBlue® Coomassie protein stain with a slow shaking overnight using 2D Rocker from Flowgen Biosciences, for getting a clear and visible band in each lane, to determine the IgG A33 hFab' molecular weight.

2.2.5 Analytical Ultracentrifugation- Sedimentation Equilibrium analysis

Analytical ultracentrifugation has 2 basic methods, which are the sedimentation equilibrium (SE) method and the sedimentation velocity (SV) method (Ralston 1993). The measurements were taken using a Beckman Optima XL-I Analytical Ultracentrifuge (Beckman Coulter, Brea, CA, USA) for both SE and SV methods. Both Rayleigh interference and UV-absorbance optical systems were used. The SV method was used to assess the homogeneity and measure the sedimentation coefficient distribution. The SE method, was utilised to measure the IgG A33 hFab' and HSA macromolecules molecular weight (Schuck et al. 2014). The centrifuge cells used in this method were constructed from sapphire windows which were sealed in an aluminium cell housing, aluminium epoxy resin centrepiece, double sectored. Additionally, 140 µl of IgG A33 hFab' and 100 µl of HSA with PBS buffer (as a reference) was taken and injected into the centrifuge-housing cells individually. After that, the centrifuge cells were loaded and balanced in a 4-hole rotor, and run at the appropriate speed at a temperature equal to $(20.0 \pm 0.1) ^\circ\text{C}$. Subsequently, the SEDFIT-MSTARv1 software (Schuck et al. 2014) was used to analyse the interference and absorbance data, for calculating the apparent weight average molecular weight $M_{w,app}$.

2.2.6 Analytical Ultracentrifugation- Sedimentation Velocity analysis

In this method, the SV was applied to assess the IgG A33 hFab' purity and the presence of dimers and aggregates, with UV-absorption optics and Rayleigh interference (Harding 2005). The IgG A33 hFab' samples were diluted from their stock solution starting from 1.20 mg/ml to 0.02 mg/ml. The centrifuge cells employed in this experiment were created from aluminium epoxy resin centrepiece, double sectored, sapphire windows which were sealed in an aluminium cell housing. Therefore, 400 µl of both IgG A33 hFab' and PBS buffer as a reference was taken and injected in the centrifuge cell housing individually. Then, the centrifuge cells were loaded and balanced in a 4-hole rotor. The Beckman Optima XL-I Analytical Ultracentrifuge instrument was calibrated at a temperature equal to $(20.0 \pm 0.1) ^\circ\text{C}$, with a speed up to 44,000 rpm. Afterwards, the SEDFIT software was used to

analyse the absorbance and interference data, to calculate the sedimentation coefficient values and distributions for each concentration.

SV was also utilised to determine the interaction between human serum albumin and IgG A33 hFab' macromolecules. The method was followed similarly as with IgG A33 hFab' SV method. However, in the SV method for investigating their interaction, the concentrations of the relative proportions for both macromolecules were (1:1), (1) for the IgG A33 hFab' only and (1) for the HSA only.

2.2.7 Ostwald (U-tube) capillary viscometer

IgG A33 hFab' and HSA macromolecules were tested to assess their molecular shape and the intrinsic viscosity, using an automated Ostwald (U-tube) capillary viscometer (Schott Geräte, Hofheim, Germany). The temperature in the water bath was controlled at (20.0°C ±0.01). In addition, at a fixed concentration of IgG A33 hFab' and series concentrations of the HSA macromolecules, five flow times (t_0) were measured to calculate the PBS buffer; also, the IgG A33 hFab' and HSA samples flow times (t) calculated with their average values for obtaining more reliable and precise results. The densities of the PBS buffer, IgG A33 hFab' and HSA samples were calculated using DMA 5000 M, Density meter, Anton Paar (Graz, Austria). The relative viscosities were obtained using the following equation (see, e.g., Gillis et al. (2014); (Harding 1997)):

$$\eta_r = \left(\frac{t}{t_0}\right) \times \left(\frac{\rho}{\rho_0}\right) \quad (3.1)$$

where, η_r is the relative viscosity of the IgG A33 hFab' and HSA sample, t is the IgG A33 hFab' and HSA solution flow time, t_0 is the PBS buffer flow time, ρ is the density of the IgG A33 hFab' and HSA solutions and ρ_0 is the density of the PBS buffer.

Afterwards, the intrinsic viscosity was calculated using the Solomon-Ciuta equation in accordance with the relative viscosity in equation (3.1) (Harding 1997):

$$[\eta] \cong \frac{\sqrt{2((\eta_r - 1) - 2 \ln(\eta_r))}}{c} \quad (3.2)$$

where, $[\eta]$ is the IgG A33 fab' and HSA intrinsic viscosity and C is the concentration in g/ml. Furthermore, $[\eta]$ from equation (3.2) was used to calculate the shape factor of the IgG A33 hFab' using the following equation (Harding 1997):

$$v = \frac{[\eta]}{v_s} \quad (3.3)$$

where, v is the viscosity increment, v_s is the “swollen” or “hydrated” specific volume for the IgG A33 or hFab' samples, i.e. swollen volume per unit anhydrous mass. For HSA, the intrinsic viscosity was evaluated using equation (3.2) and the following equations (see Harding (1997); (Jiwani et al. 2020)):

$$\eta_{red} = [\eta] \cdot (1 + K_H [\eta] c) \quad (3.4)$$

$$\frac{(\ln \eta_r)}{c} = [\eta] (1 - K_K [\eta] c) \quad (3.5)$$

where, η_{red} is the reduced viscosity, K_H Huggins constant, K_k Kraemer constant.

3. Results and Discussion

3.1 Producing a pure sample of IgG A33 hFab' and HSA through dialysis and with their concentration measurements

Human serum albumin and IgG A33 hFab' macromolecules were dialysed before measuring their concentrations. The dialysis experiment aimed to purify the contents of the dialysis tubing from the impurities and salts such as NaCl. The results of pre-and post-dialysis were the concentration for the IgG A33 hFab' decreased but human serum albumin increased. Table 1 shows the concentrations of HSA and IgG A33 hFab' macromolecules were taken after running the dialysis experiment.

Table 1: The average absorbance and concentration of IgG A33 hFab' and HSA with their standard deviation, using a UV spectrophotometer for five measurements.

Measurement /Average	Macromolecules name	Absorbance (A)	C (mg/ml)
Measurement (1)	IgG A33 hFab'	0.352	1.285
Measurement (2)	IgG A33 hFab'	0.353	1.288
Measurement (3)	IgG A33 hFab'	0.355	1.296
Measurement (4)	IgG A33 hFab'	0.356	1.299
Measurement (5)	IgG A33 hFab'	0.357	1.303
Average	-	0.355 (± 0.002)	1.294 (± 0.008)
Measurement (1)	HSA	0.839	3.119
Measurement (2)	HSA	0.838	3.115
Measurement (3)	HSA	0.836	3.108
Measurement (4)	HSA	0.835	3.104
Measurement (5)	HSA	0.835	3.104
Average	-	0.8366 (± 0.0018)	3.110 (± 0.007)

Table 1 illustrates the absorbance values obtained from the UV spectrophotometer using equation (1) (see section 2.2.2). As shown in Table 1, the concentration of IgG A33 hFab' was confirmed = $(1.29 \pm 0.01) \text{ mg.ml}^{-1}$. Also, the HSA concentration was

= (3.11 ± 0.01) mg.ml⁻¹. The linearity relation between absorbance and concentration values was confirmed by Gobrecht et al. (2015).

3.2 Homogeneity/heterogeneity evaluation with dynamic light scattering

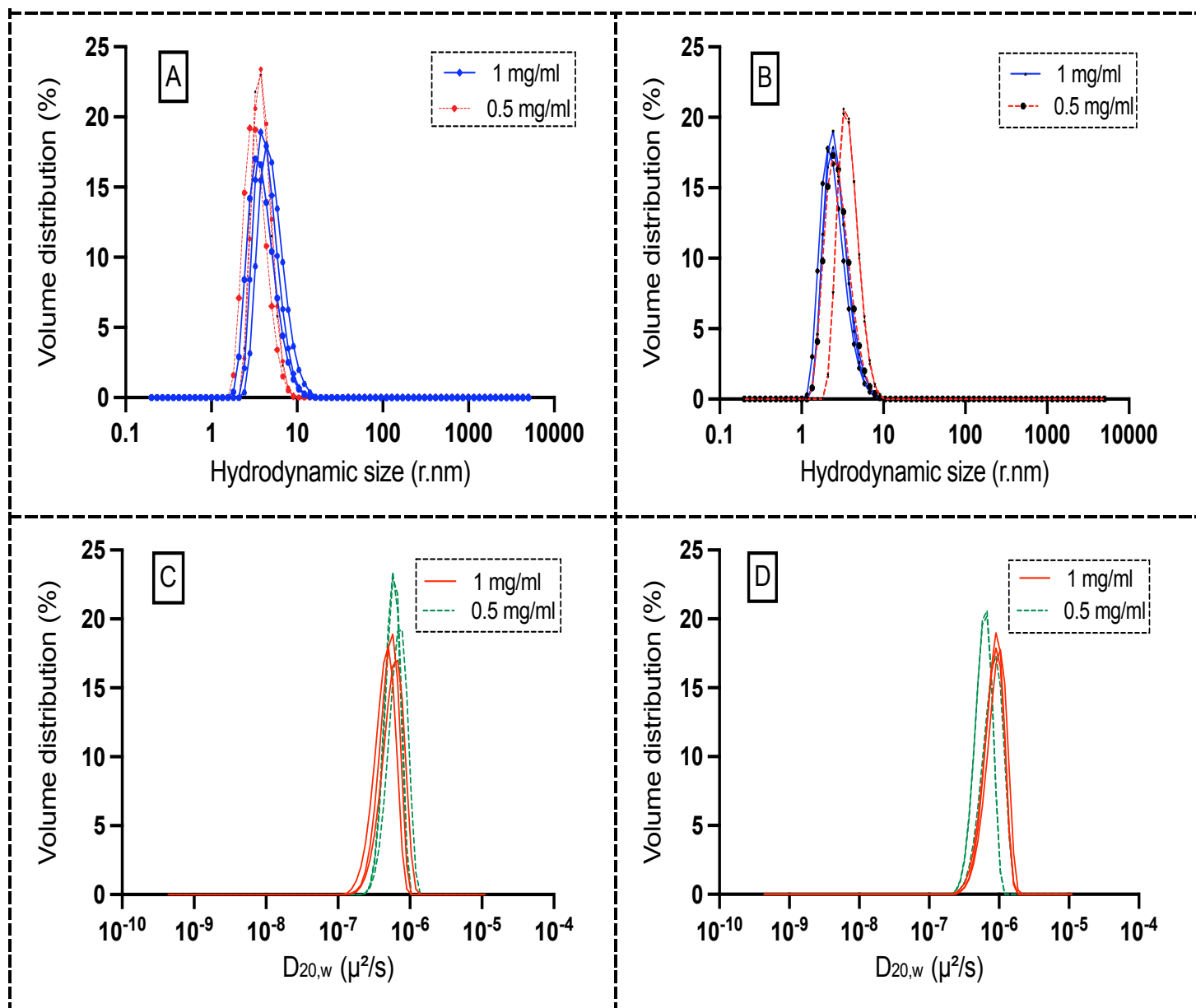


Figure 3: Dynamic light scattering method of IgG A33 hFab' macromolecule. Each one of the above diagrams; A, B, C and D represents multiple measurements of the volume distribution (%) as a function of hydrodynamic size (r.nm) and the diffusion coefficient, $D_{20,w}$ ($\frac{\mu^2}{s}$) for dual angles at 20.0 ° C. The scattering angles for plots **A**

and **C** were measured using 13° forwardscatter. In contrast, the scattering angles for plots **B** and **D** were measured using 173° backscatter.

The dynamic light scattering experiment represents a viable method for determining the IgG A33 hFab' macromolecule heterogeneity state. Of particular interest, Figures (3, A and B) showed that the IgG A33 hFab' macromolecule narrow in distribution sizes when changing the concentrations among 0.5 mg/ml and 1 mg/ml by using both 13° forwardscatter and 173° backscatter angles. The hydrodynamic diameters for the IgG A33 hFab' macromolecule confirmed from Figure (3-A) that 0.5 mg/ml had ~ 3 nm and 1 mg/ml had ~ 3.5 nm in size. Also, the results of IgG A33 hFab' macromolecule in Figure (3-B) proved that 0.5 mg/ml had ~ 2.4 nm and 1 mg/ml had ~ 1.9 nm in size. These findings indicate that the IgG A33 hFab' macromolecule with PBS buffer was pure and free of aggregated particles. Furthermore, the state of aggregated particles and turbidity state was shown regarding IgG A33 hFab' macromolecule with isopropyl alcohol preparation in the Appendix section, (Figures 1 and 2).

On the other hand, Figures (3, C and D) gave more information concerning the diffusion coefficients ($D_{20,w}$) using 13° forwardscatter and 173° Backscatter angles. The lower diffusion coefficient correlated with no aggregation of IgG A33 hFab' macromolecule. The diffusion coefficient results confirmed from Figure (3-C) that 0.5 mg/ml had $\sim 6.9 \times 10^{-7} \left(\frac{\mu^2}{s}\right)$ and 1 mg/ml had $5.9 \times 10^{-7} \left(\frac{\mu^2}{s}\right)$. Further, the results of Figure (3-D) illustrated that 0.5 mg/ml had $\sim 7.3 \times 10^{-7} \left(\frac{\mu^2}{s}\right)$ and 1 mg/ml had $9.5 \times 10^{-7} \left(\frac{\mu^2}{s}\right)$. Together these results provide important insight, that there is no evidence of aggregation and turbidity.

3.3 Molecular weight measurements

3.3.1 Sodium Dodecyl Sulphate – Polyacrylamide Gel Electrophoresis

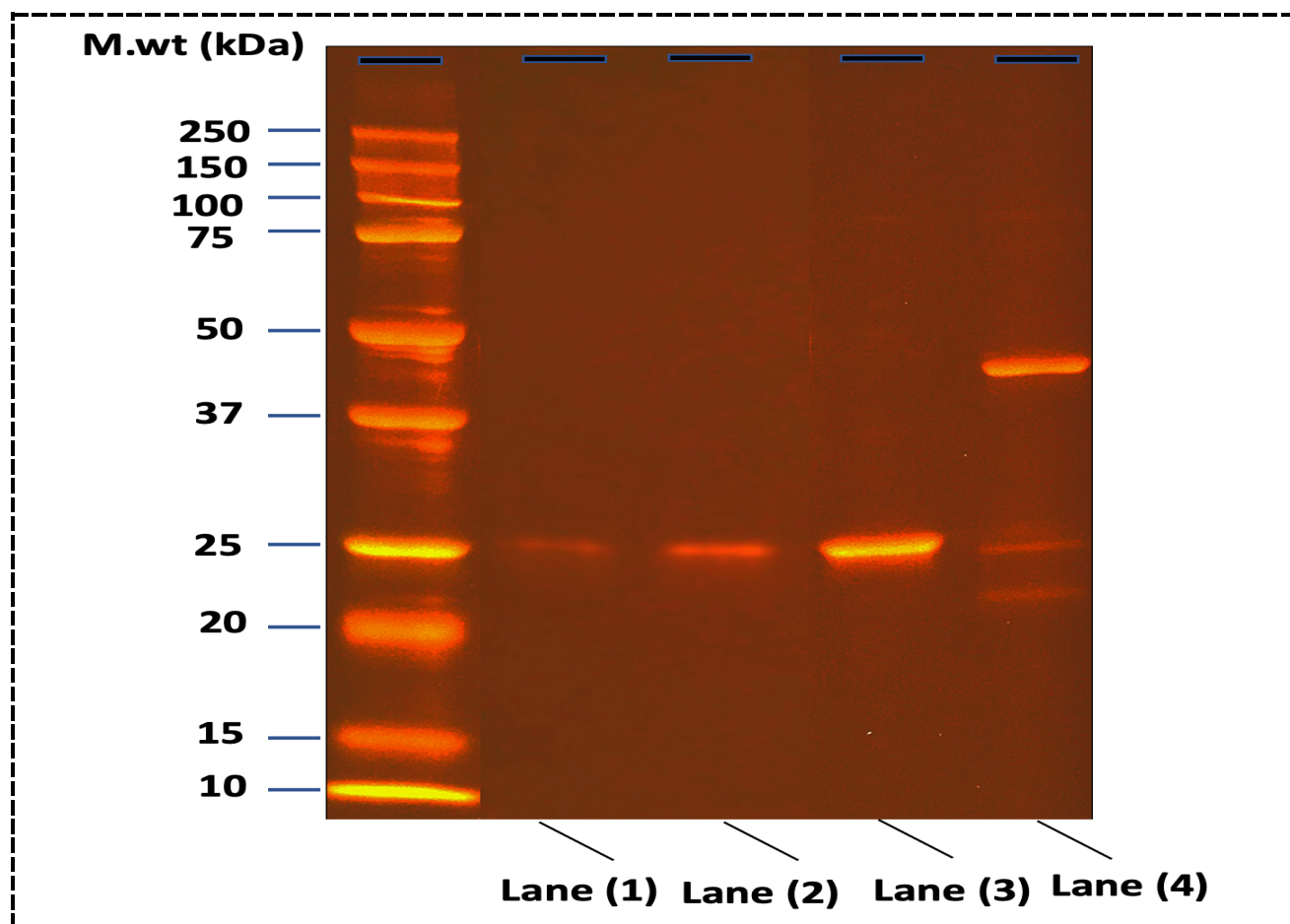


Figure 4: SDS-PAGE determination of IgG A33 hFab' molecular weight (M.wt) in the range of 10 – 250 kDa as a marker lane. A reducing agent called 2-mercaptoethanol was used in lanes (1,2 and 3) with different concentrations. Lane (4) was run without applying 2-mercaptoethanol, on a 12% gel (30 μ l/well) stained with InstantBlue[®] Coomassie protein stain. The false colour in this plot was created using ImageJ software (Rasband 2011).

For the molecular weight measurements of the IgG A33 hFab' sodium dodecyl sulfate - polyacrylamide gel electrophoresis (SDS-PAGE) was first used. Figure 4 presents the results obtained before and after applying 2-Mercaptoethanol with a series of concentrations in lanes (1,2 and 3). It is obvious from Figure 4 that the molecular weight of IgG A33 hFab' macromolecule in lane 1,2 and 3 was ~ 25 kDa.

In contrast, line 4 showed the molecular weight was ~ 48 kDa. The SDS-PAGE experiment confirmed is consistent with that of Lu et al. (2008) experimental results on “solution conformation of antibody fragments” study, which showed that the Human $\gamma 1$ Fab' molecular weight is 48 kDa, as well. Since the number of cystine residues in IgG A33 hFab' macromolecule are 11 residues (King et al. 2001), the disulfide bonds acting as a bridge between the heavy and light chains. Interestingly, the most striking result to emerge is that the using of reducing conditions like 2-mercaptoethanol, will break the disulfide bonds and make the molecular weight lower as shown in lanes 1,2 and 3. Therefore, as shown in lane (4), the IgG A33 hFab' macromolecule is ~ 48 kDa, which means a monomeric macromolecule state. The next step was to perform sedimentation equilibrium analysis to measure the molecular weight in free solution in the absence of SDS detergent.

3.3.2 Analytical Ultracentrifugation- Sedimentation Equilibrium

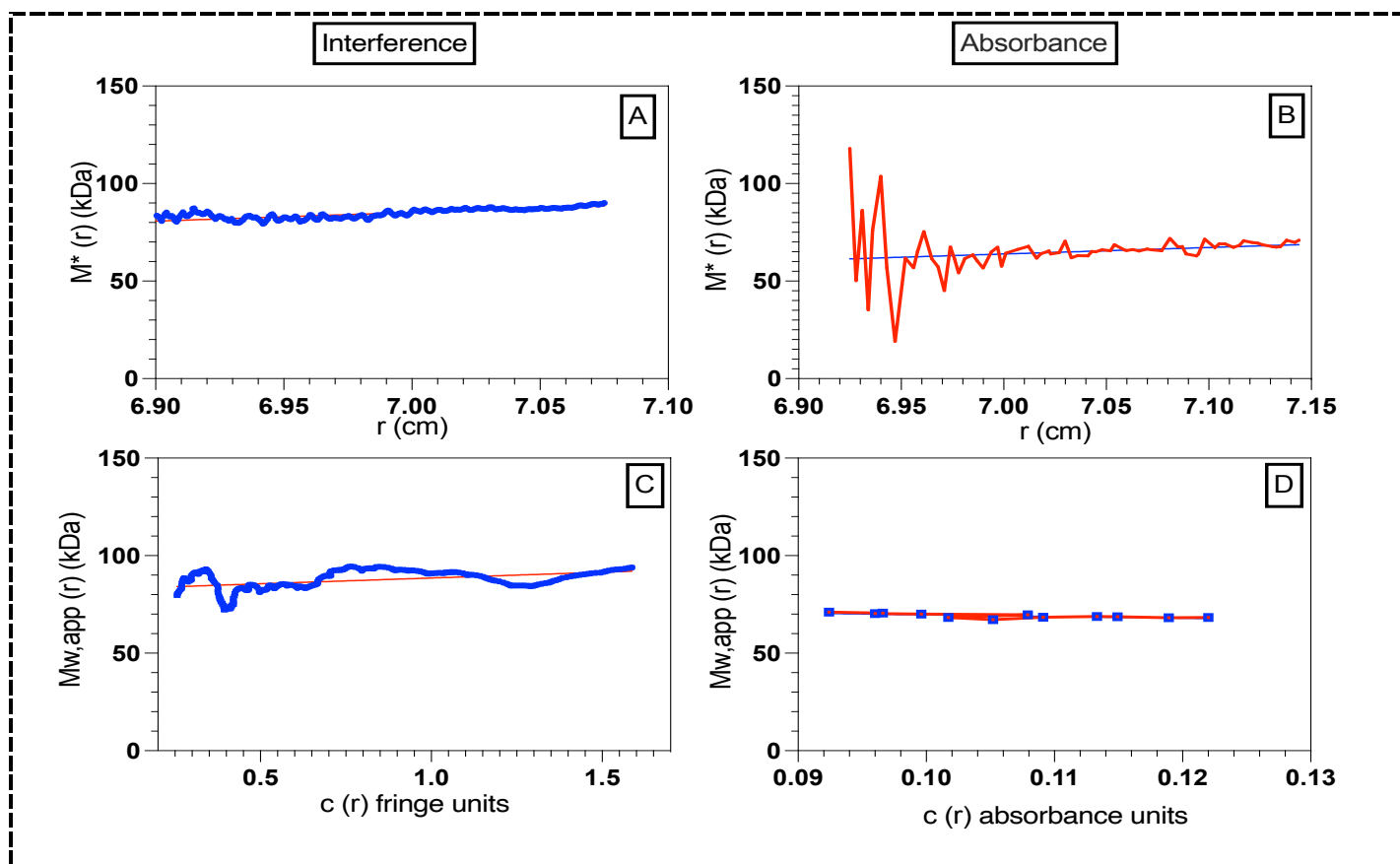


Figure 5: Sedimentation equilibrium of HSA, 2 methods of analysis are used in the SEDFIT-MSTAR program– the M^* extrapolation method (A and B) and the hinge method (C and D) (Schuck et al. 2014). A & C are using interference optics and B & D are using absorption optics at 280nm. A loading concentration of 0.6 mg.ml^{-1} was used at 20.0°C .

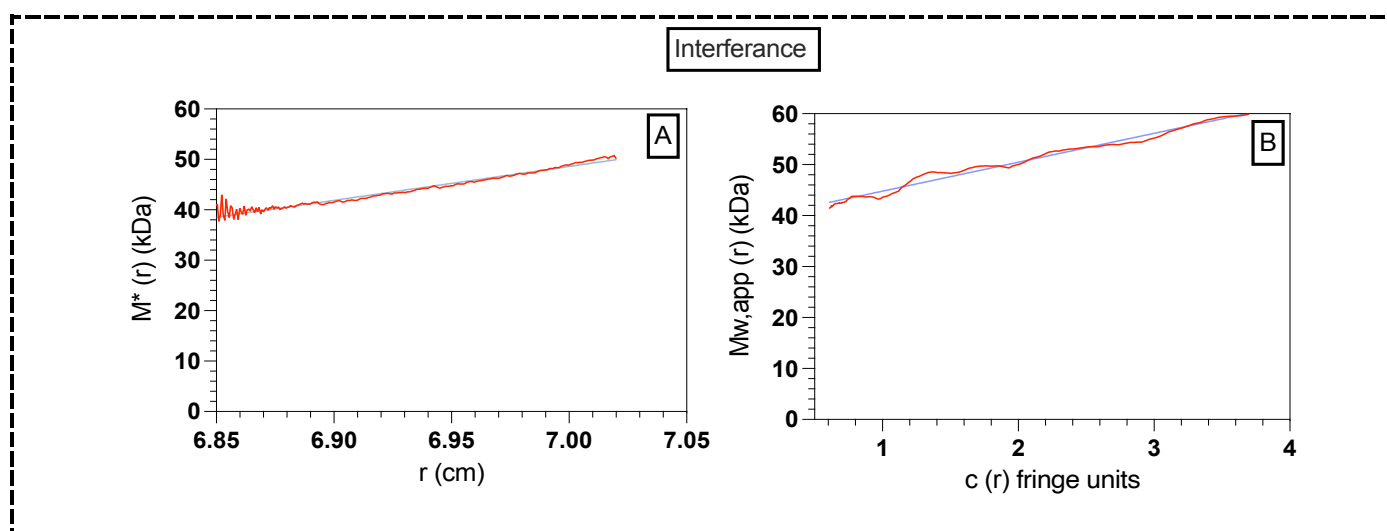
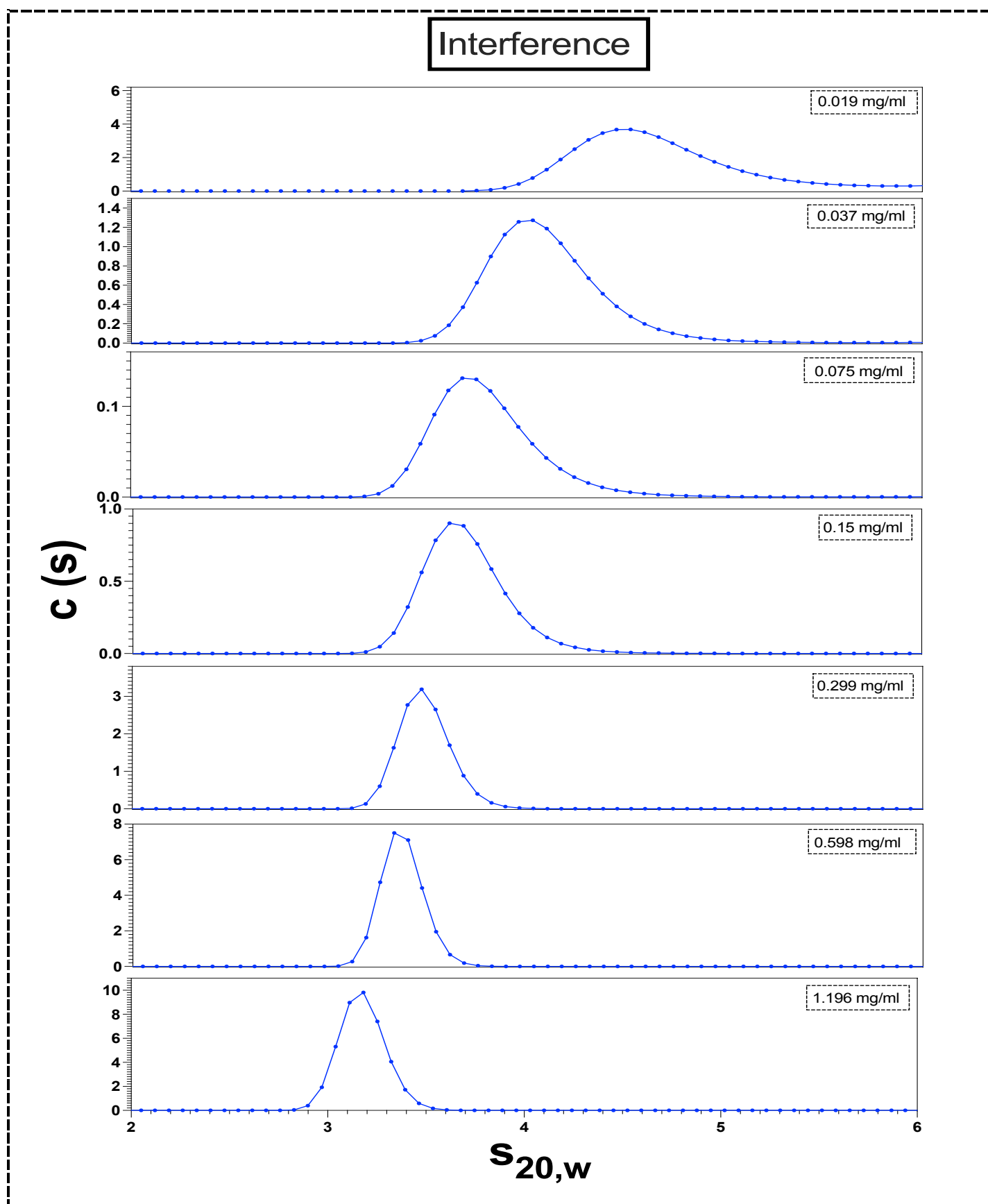


Figure 6: Sedimentation equilibrium analysis of IgG A33 hFab' using SEDFIT-MSTAR (Schuck et al. 2014). Using (A) the M^* extrapolation method and (B) hinge point method, with concentrations expressed in fringe units, a loading concentration of 0.62 mg/ml was used.

Sedimentation equilibrium was employed to assess the HSA and IgG A33 hFab' macromolecules apparent molecular weight ($M_{w,app}$) using SEDFIT-MSTARv1 software (Schuck et al. 2014). The diagrams in Figures (5 and 6), clarifies the determination of the apparent molecular weight of the HSA and IgG A33 hFab' macromolecules at 0.60 mg/ml and 0.62 mg/ml, respectively. At these low concentrations, non-ideality effects were considered to be small. Accordingly, the absorbance results in Figure (5-B+D) revealed that the HSA molecular weight utilising M^* method is $\approx (70.9 \pm 0.3)$ kDa and the $M_{w,app}$ (hinge) method is $\approx (70.5 \pm 0.3)$ kDa, consistent with a monomeric protein (Belinskaia et al. 2021). With the interference results a slightly higher molecular weight was obtained: $M_{w,app}$ is $\approx (86.0 \pm 4.0)$ kDa with both the M^* and hinge methods.

For IgG A33 hFab' the interference data in Figure (6-A+B), showed that IgG A33 hFab' molecular weight employing M^* method is $\approx (51.9 \pm 1.4)$ kDa and hinge method is $\approx (49.9 \pm 1.4)$ kDa, and similar results were obtained with UV absorption optics at 280nm.

3.4 The assessment of purity and the presence of dimers and aggregates



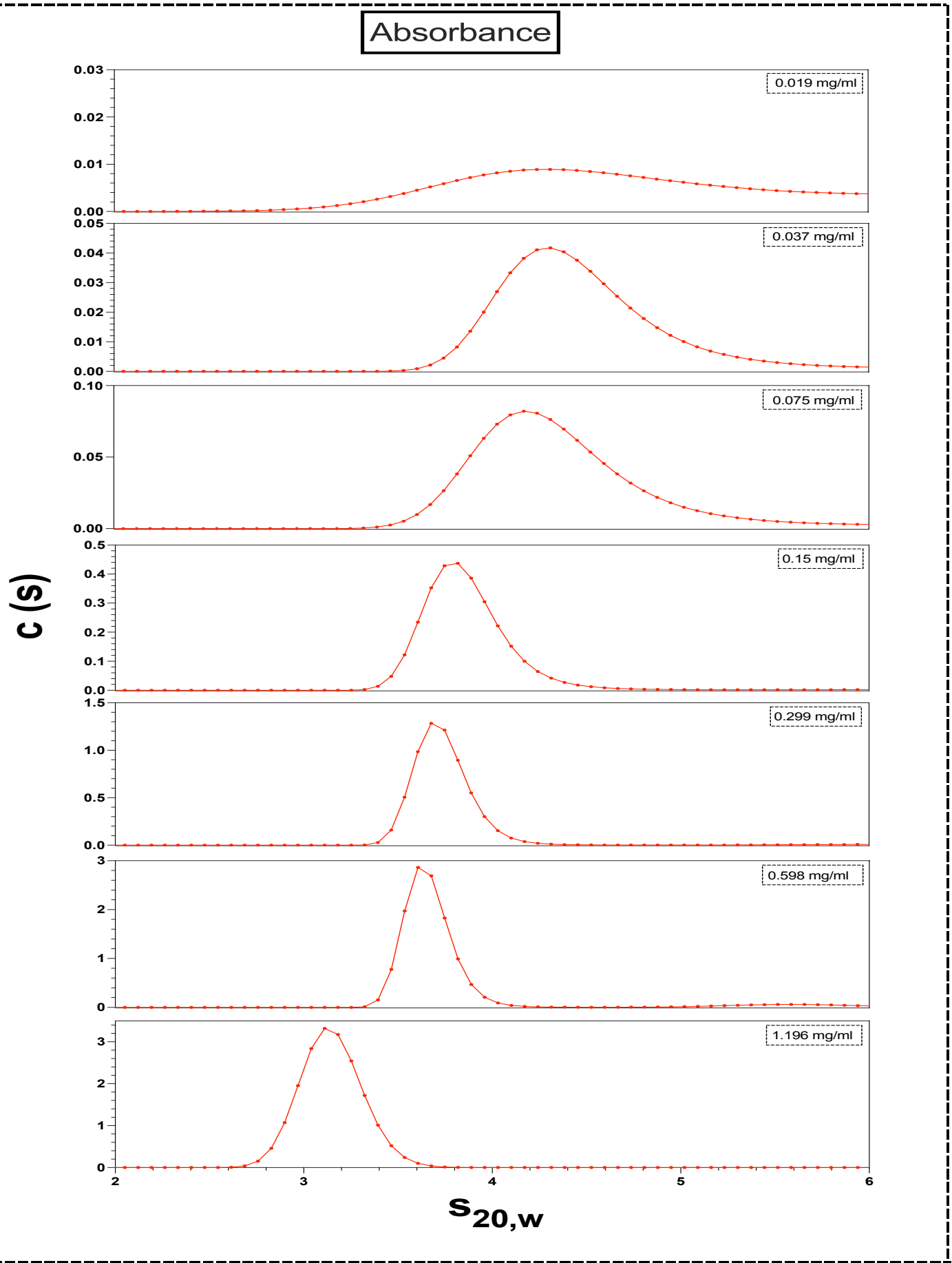


Figure 7: The $c(s)$ profile for IgG A33 hFab' macromolecule as a function of the sedimentation coefficient distribution ($s_{20,w}$) at 7 serial dilutions, starting from 1.2 mg/ml to 0.02 mg/ml, for both interference measurements (—●—) and the absorbance measurements (—●—) at 20.0 °C.

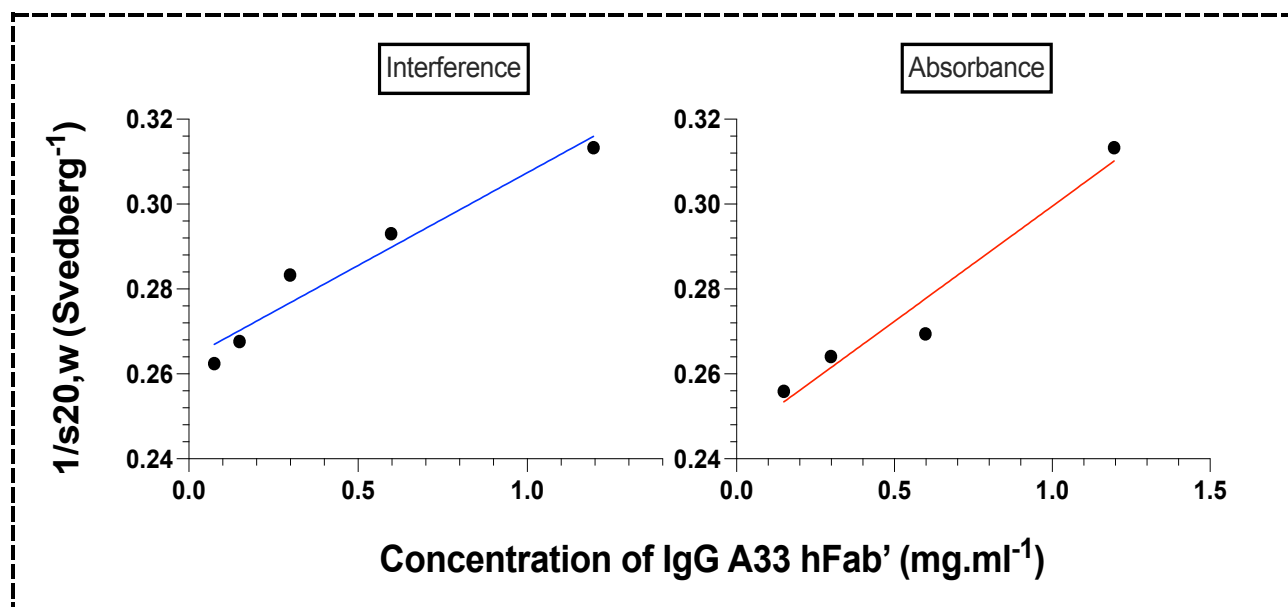


Figure 8: Reciprocal diagrams of $s_{20,w}$ (s⁻¹ or Svedberg⁻¹) versus the concentration of IgG A33 hFab' macromolecule in (mg/ml), and with extrapolation to zero concentration at 20.0 °C. $s_{20,w}^0 = 3.8$ S (interference) and 4.1 S (absorbance).

Sedimentation Velocity (SV) was applied to assess the presence of aggregates and dimers using the interference and absorbance optical methods. As noticed from Figure (7), the $c(s)$ profile versus $s_{20,w}$ was utilised for both Rayleigh interference and the absorbance methods. Accordingly, the results of IgG A33 hFab' macromolecule is pure and free of aggregated particles. This was evidenced by the existence of one peak in the interference and absorbance data for a series of concentrations starting from 1.12 mg/ml to 0.02 mg/ml.

Afterwards, the illustration in Figure (8), shows the reciprocal of IgG A33 hFab' macromolecule sedimentation coefficient ($1/s_{20,w}$), which generated by the extrapolation to zero concentration, for eliminating the non-ideality against the concentration in mg/ml. The extrapolated $1/s_{20,w}^0$ values of the interference and absorbance data are 0.2637 Svedberg⁻¹ and 0.2453 Svedberg⁻¹, respectively. This

gives corresponding $s_{20,w}^0$ values of 3.79 Svedberg (interference) and 4.07 Svedberg (absorbance), in agreement with Carrasco et al. (1999). It seems that the IgG A33 hFab' is monomeric, homogeneous and free of aggregated macromolecules by the existing of one peak for both interference and absorbance data. Also, since the state of the IgG A33 hFab' macromolecule was confirmed monomeric using SDS-PAGE method, therefore, the monomeric state will allow us to investigate more using the SV of possible interactions of the IgG A33 hFab' with human serum albumin.

3.5 Investigating a possibility of HSA and IgG A33 hFab' interactions

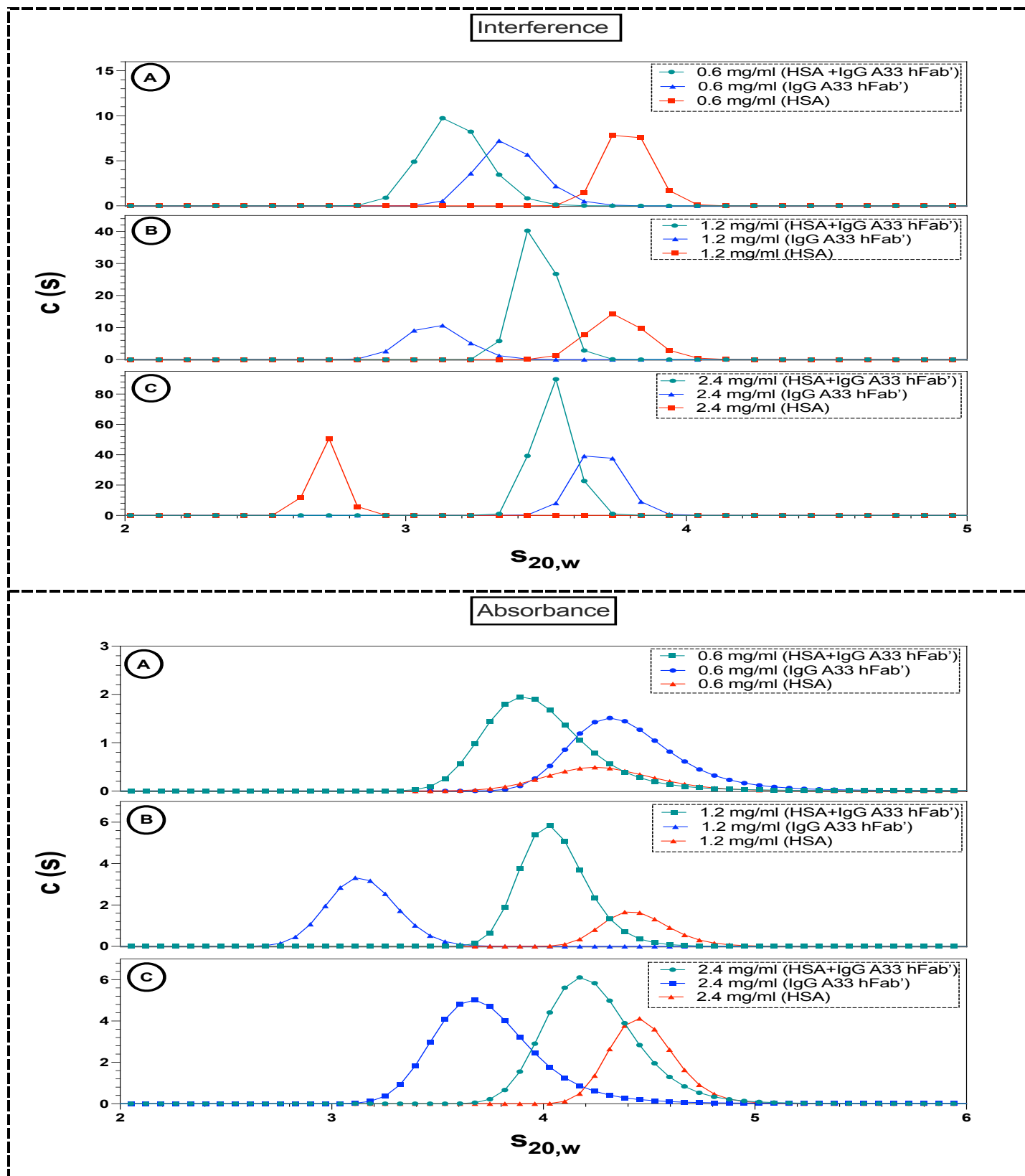





Figure 9: Sedimentation velocity (SV) analysis for HSA (, IgG A33 hFab' () and a mixture of the two () at differing mixing ratios. Interference and absorbance (280 nm) records shown.

A further application of SV was to investigate the possible interactions between the HSA and the IgG A33 hFab' macromolecules. HSA and IgG A33 hFab' using both interference and absorbance optical systems with different concentrations, which are 0.6 mg/ml (Figure 9-A), 1.2 mg/ml (Figure 9-B) and 2.4 mg/ml (Figure 9-C). Only one peak is seen in the mixtures suggesting a possible interaction, although this single peak has a sedimentation coefficient lower than the HSA – if an interaction has taken place, the complex must have a much higher asymmetry to explain the slower sedimentation coefficient (as normally a larger molecule would sediment faster). The appearance of a single peak may however possibly be explained by the Johnston and Ogston (1946) effect. The faster moving HSA may be being slowed down by having to move through the slower moving IgG A33 hFab'. According to the estimation of refractive increment boundaries, there is an apparent rise in the quantity of the less rapidly sedimenting composition with a corresponding reduction in the amount of other compositions. The impact is minimal at low protein concentrations, but it constantly rises as the concentration is increased. This is clearly a matter of further research.

3.6 The analysis of the viscosity

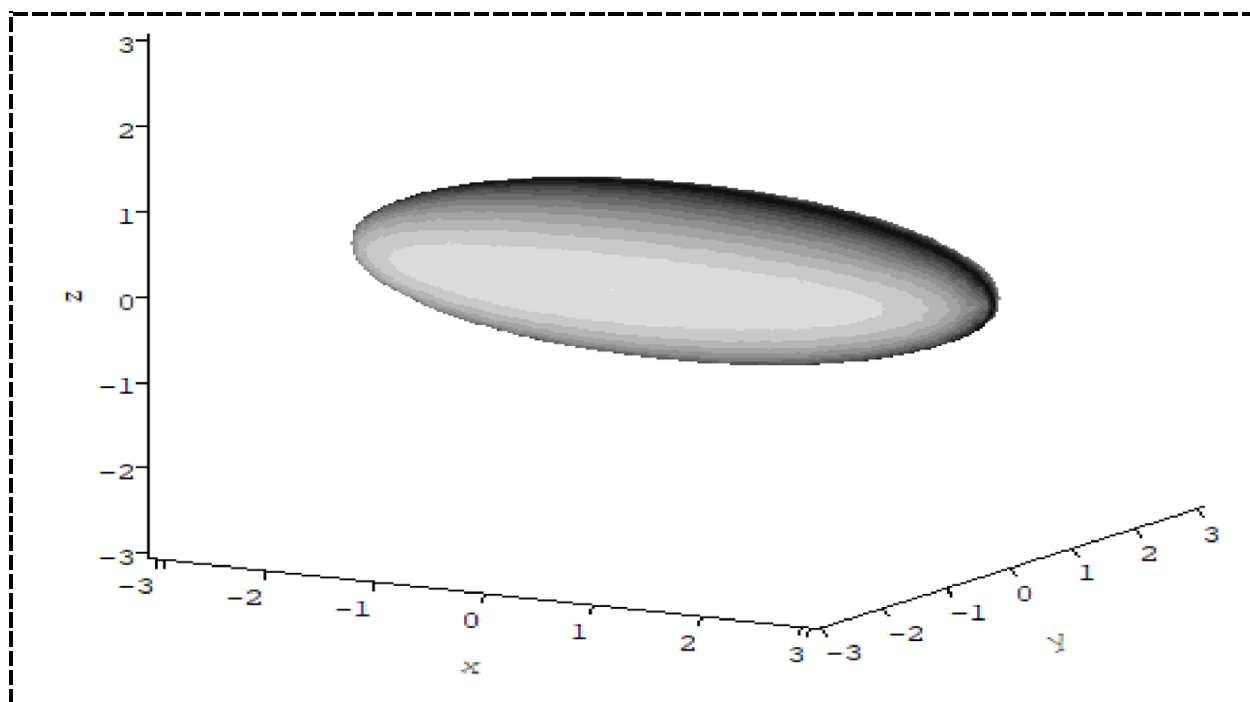


Figure 10: Ellipsoidal (prolate) representation of the IgG A33 hFab' macromolecule from the hydrodynamic analysis generated using ELLIPS 1 software. The axial ratio $a/b = 2.9$ and $b/c = 1.00$.

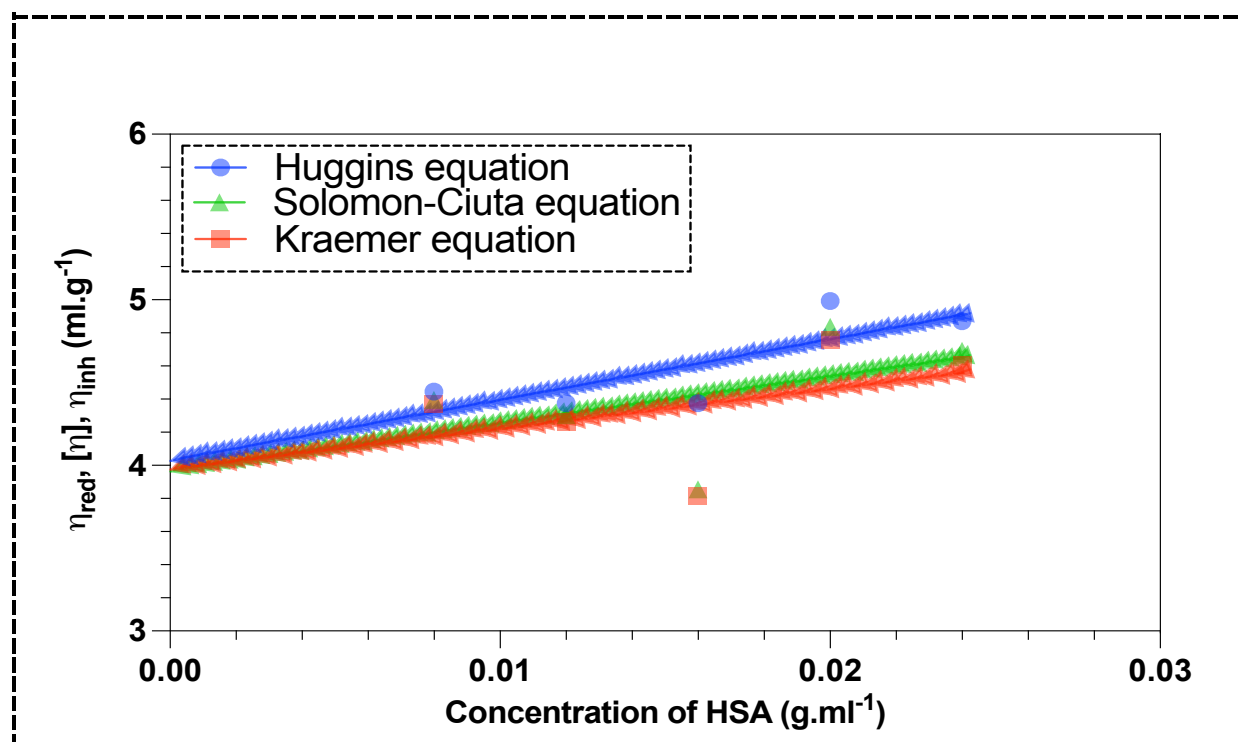


Figure 11: The intrinsic viscosity of human serum albumin plot using multiple viscosity functions. [—●—]: is the reduced viscosity (η_{red}) fitted by Huggins equation; [—▲—] is the fitting of Solomon-Ciuta estimates equation ($[\eta]$); [—■—] is the inherent viscosity (η_{inh}) fitted by Kraemer equation with a linear extrapolation to zero concentration.

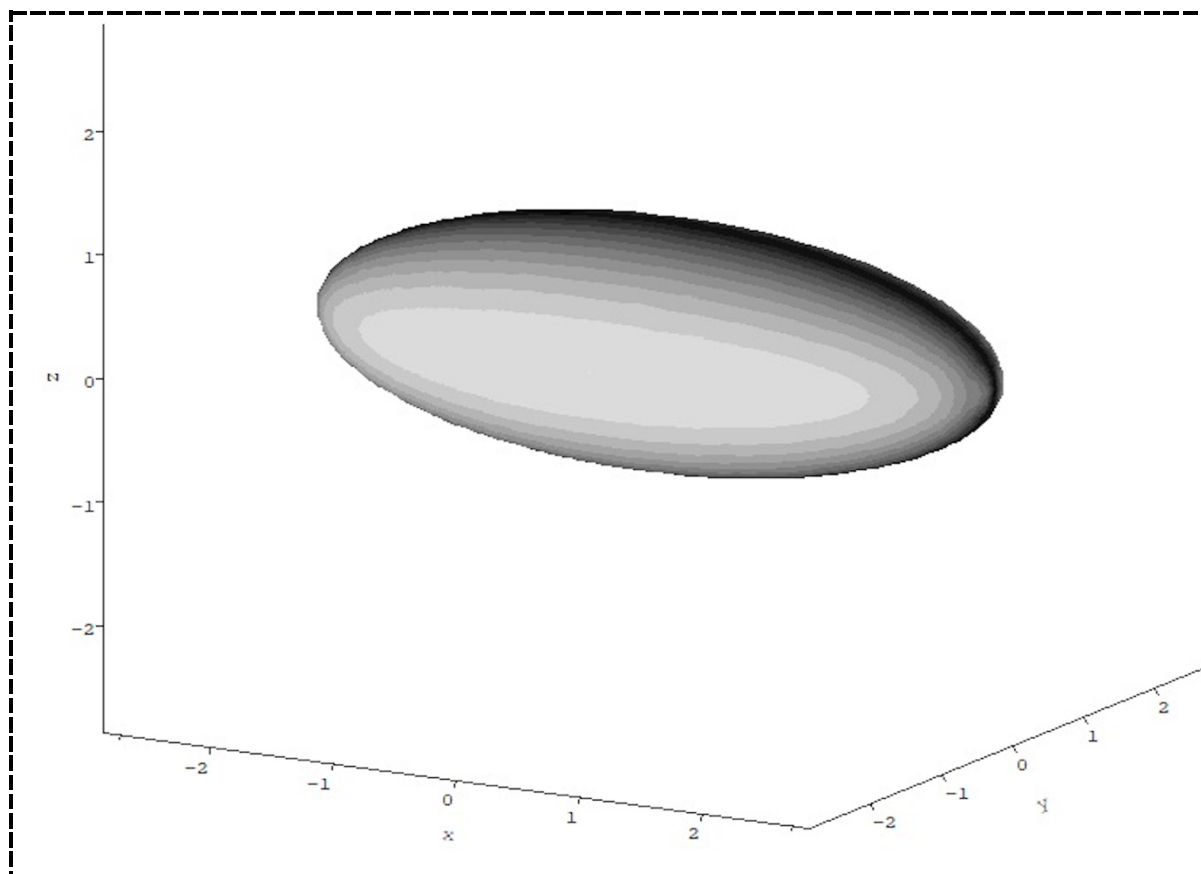


Figure 12: Ellipsoidal (prolate) representation of the HSA macromolecule from the hydrodynamic analysis generated using ELLIPS 1 software. The axial ratio $a/b = 2.7$ and $b/c = 1.00$.

Table 2: Summary of IgG A33 hFab' and HSA hydrodynamic properties.

Macromolecules properties	IgG A33 hFab'	HSA
\bar{v}	0.731 ml/g	0.736 ml/g
δ	0.3583 g/g	0.4117 g/g
v_s	1.09 ml/g	1.15 ml/g
ϵ_{280}	1394 ml.g ⁻¹ .cm ⁻¹	526 ml.g ⁻¹ .cm ⁻¹
$[\eta]$	3.95 ml/g	3.99 ml/g

v	3.62	3.47
a/b (prolate)	2.9	2.7
$s^{\circ}_{20,w}$	3.95	N.D
M_w (SDS-PAGE)	48 kDa	N.D
M_w (Sedimentation equilibrium)	50.9 kDa	70.7 kDa

The Ostwald (U-tube) capillary viscometer is a fundamental instrument for validation of the IgG A33 hFab' and HSA macromolecules shape and to determine their intrinsic viscosities. The results shown that HSA has ~ the same intrinsic viscosity as IgG A33 hFab' calculated using (equation 3.2 for the HSA), with an average value getting from using equations (3.2.3.4 and 3.5) for the HSA (see Materials and methods section). According to Figures 10 and 12, the ellipsoidal (prolate) representation with a/b seems to be similar: the shape factor of the HSA is approximately the same as with IgG A33 hFab', which were found from ELLIPS1 software (see Figures 10 and 12). From table 2, the extinction coefficient of IgG A33 hFab' has a higher value than the HSA, this is referred to the existing of highly amounts of tryptophan and tyrosine amino acid residues. The PERKINS software was employed and gave the partial specific volume (\bar{v}) and hydration (δ) values of both macromolecules depending on their amino acid sequences, which shown in table 2, as well. Further, the intrinsic viscosity of HSA was calculated after measuring a series of HSA concentrations at a constant temperature of $(20.00 \pm 0.01) ^\circ\text{C}$. However, the non-ideality was eliminated by extrapolation to zero concentrations (see. e.g., Chun et al. (2020)) review article.

4. Conclusions and Future Work

In conclusion, this experimental study has set out to characterise the IgG A33 hFab' and human serum albumin macromolecules using several hydrodynamic techniques, alongside the investigation of possible interactions between them. The investigation by both dynamic light scattering, and sedimentation velocity has revealed that IgG A33 hFab' can be used PBS buffer as an aqueous solvent, which is homogeneous and free of aggregated particles. This study has found that the IgG A33 hFab' molecular weight is ~ 48- 50 kDa and is in the monomeric state using the SDS-PAGE and SE methods. Application of reducing conditions namely 2-mercaptoethanol reduces the M.wt from 48 kDa to 25 kDa, by the breakage in the disulfide bonds. The HSA molecular weight is 71 kDa through applying the SE method, as well and sedimentation velocity also shows this to be homogeneous (one peak). The SV results supported the SDS-PAGE and SE results, since the IgG A33 hFab' and HSA are monomeric and homogenous by the existence of one peak for a series of concentrations. The SV method was also used as a for a preliminary investigation in the possible interaction between HSA and IgG A33. The existence of a single peak in the mixture may be due to an interaction or due to a phenomenon known as the Johnston-Ogston effect: this is a matter for follow up/ further investigation. This means if there is an interaction this will limit the use of IgG A33 hFab' as a biotherapeutic drug. Further experimental investigations are therefore needed using Sedimentation Equilibrium to verify the Sedimentation Velocity findings concerning the potential interaction between HSA and IgG A33 hFab' macromolecules, to see the combined molecular will be together.

List of references

- BELINSKAIA, D. A., VORONINA, P. A., BATALOVA, A. A. & GONCHAROV, N. V. 2021. Serum Albumin. *Encyclopedia*, 1(1), 65-75.
- CARRASCO, B., DE LA TORRE, J. G., BYRON, O., KING, D., WALTERS, C., JONES, S. & HARDING, S. E. 1999. Novel size-independent modeling of the dilute solution conformation of the immunoglobulin IgG Fab' domain using SOLPRO and ELLIPS. *Biophysical journal*, 77(6), 2902-2910.
- CHUN, T., MACCALMAN, T., DINU, V., OTTINO, S., PHILLIPS-JONES, M. K. & HARDING, S. E. 2020. Hydrodynamic Compatibility of Hyaluronic Acid and Tamarind Seed Polysaccharide as Ocular Mucin Supplements. *Polymers*, 12(10), 2272.
- GILLIS, R. B., ROWE, A. J., ADAMS, G. G. & HARDING, S. E. 2014. A review of modern approaches to the hydrodynamic characterisation of polydisperse macromolecular systems in biotechnology. *Biotechnology and Genetic Engineering Reviews*, 30(2), 142-157.
- GOBRECHT, A., BENDOULA, R., ROGER, J.-M. & BELLON-MAUREL, V. 2015. Combining linear polarization spectroscopy and the Representative Layer Theory to measure the Beer–Lambert law absorbance of highly scattering materials. *Analytica chimica acta*, 853, 486-494.
- HARDING, S. E. 1994. Determination of diffusion coefficients of biological macromolecules by dynamic light scattering. *Methods in Molecular Biology*, 22, 75-84.
- HARDING, S. E. 1997. The intrinsic viscosity of biological macromolecules. Progress in measurement, interpretation and application to structure in dilute solution. *Progress in biophysics and molecular biology*, 68(2), 207-262.
- HARDING, S. E. 2005. Analysis of polysaccharides size, shape and interactions. *Analytical ultracentrifugation techniques and methods*, 231-252.
- JIWANI, S. I., GILLIS, R. B., BESONG, D., ALMUTAIRI, F., ERTEN, T., KÖK, M. S., HARDING, S. E., PAULSEN, B. S. & ADAMS, G. G. 2020. Isolation and Biophysical Characterisation of Bioactive Polysaccharides from Cucurbita Moschata (Butternut Squash). *Polymers*, 12(8), 1650.
- JOHNSTON, J. & OGSTON, A. 1946. A boundary anomaly found in the ultracentrifugal sedimentation of mixtures. *Transactions of the Faraday Society*, 42, 789-799.
- KING, D. J., ADAIR, J. R. & OWENS, R. J. 2001. Humanized antibodies directed against A33 antigen. Google Patents.
- LU, Y., HARDING, S. E., TURNER, A., SMITH, B., ATHWAL, D. S., GROSSMANN, J. G., DAVIS, K. G. & ROWE, A. J. 2008. Effect of PEGylation on the solution conformation of antibody fragments. *Journal of pharmaceutical sciences*, 97(6), 2062-2079.
- RALSTON, G. B. 1993. *Introduction to analytical ultracentrifugation*, Beckman California.
- RASBAND, W. S. 2011. Imagej, US National Institutes of Health, Bethesda, Maryland, USA. <http://imagej.nih.gov/ij/>.
- SAND, K. M. K., BERN, M., NILSEN, J., NOORDZIJ, H. T., SANDLIE, I. & ANDERSEN, J. T. 2015. Unraveling the interaction between FcRn and albumin: opportunities for design of albumin-based therapeutics. *Frontiers in immunology*, 5, 682.
- SCHUCK, P., GILLIS, R. B., BESONG, T. M., ALMUTAIRI, F., ADAMS, G. G., ROWE, A. J. & HARDING, S. E. 2014. SEDFIT–MSTAR: molecular weight and molecular weight distribution analysis of polymers by sedimentation equilibrium in the ultracentrifuge. *Analyst*, 139(1), 79-92.
- SWINEHART, D. F. 1962. The beer-lambert law. *Journal of chemical education*, 39(7), 333.

- WALSH, G. 2014. Biopharmaceutical benchmarks 2014. *Nature biotechnology*, 32(10), 992-1000.
- XENAKI, K. T., OLIVEIRA, S. & VAN BERGEN EN HENEGOUWEN, P. M. 2017. Antibody or antibody fragments: implications for molecular imaging and targeted therapy of solid tumors. *Frontiers in immunology*, 8, 1287.
- ZEESHAN, F., MADHESWARAN, T., PANNEERSELVAM, J., TALIAN, R. & KESHARWANI, P. 2021. Human serum albumin as multifunctional nanocarrier for cancer therapy. *Journal of Pharmaceutical Sciences*, 110(9), 3111-3117.

Appendix: Investigation of the effect of a non-aqueous solvent (isopropyl alcohol) on the properties of IgG A33 hFab'

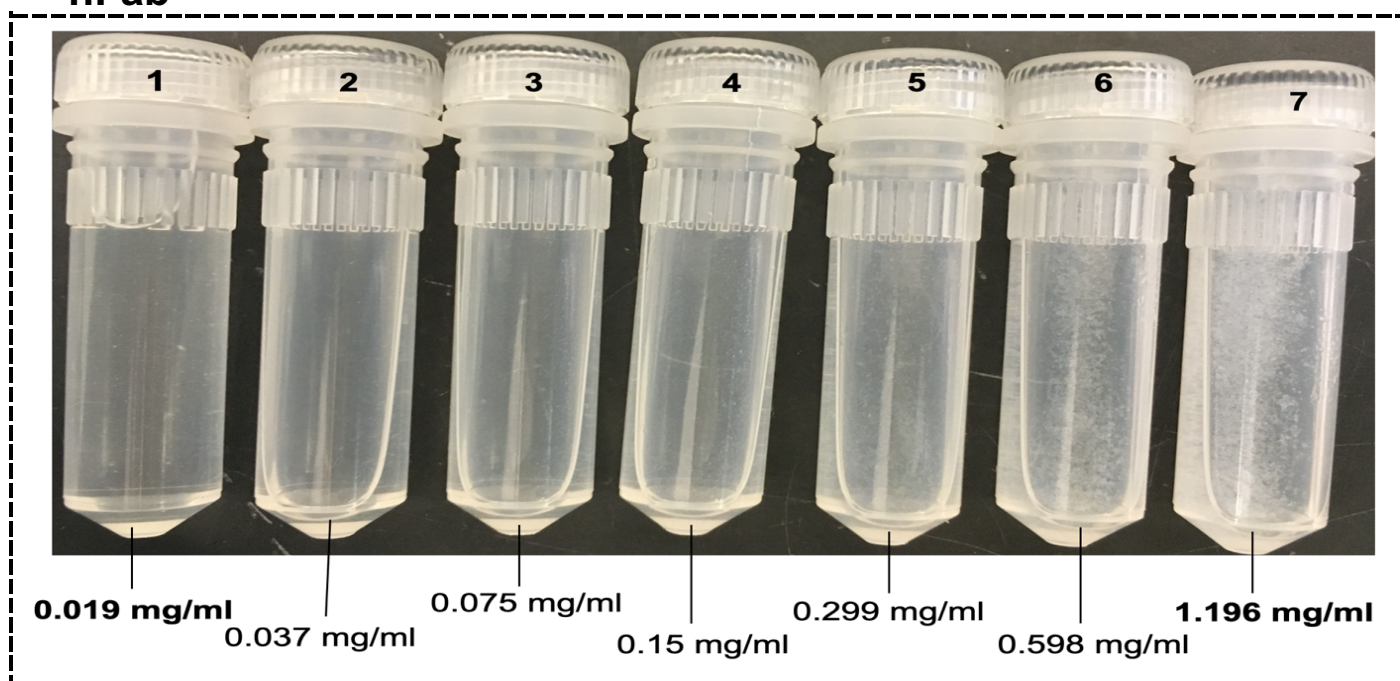


Figure (A1): Representative selection of Eppendorf tubes showing the increasing in turbidity or aggregation of the IgG A33 hFab' with isopropyl alcohol starting from tube number (1) 0.019 mg/ml to tube number (7) 1.196 mg/ml.

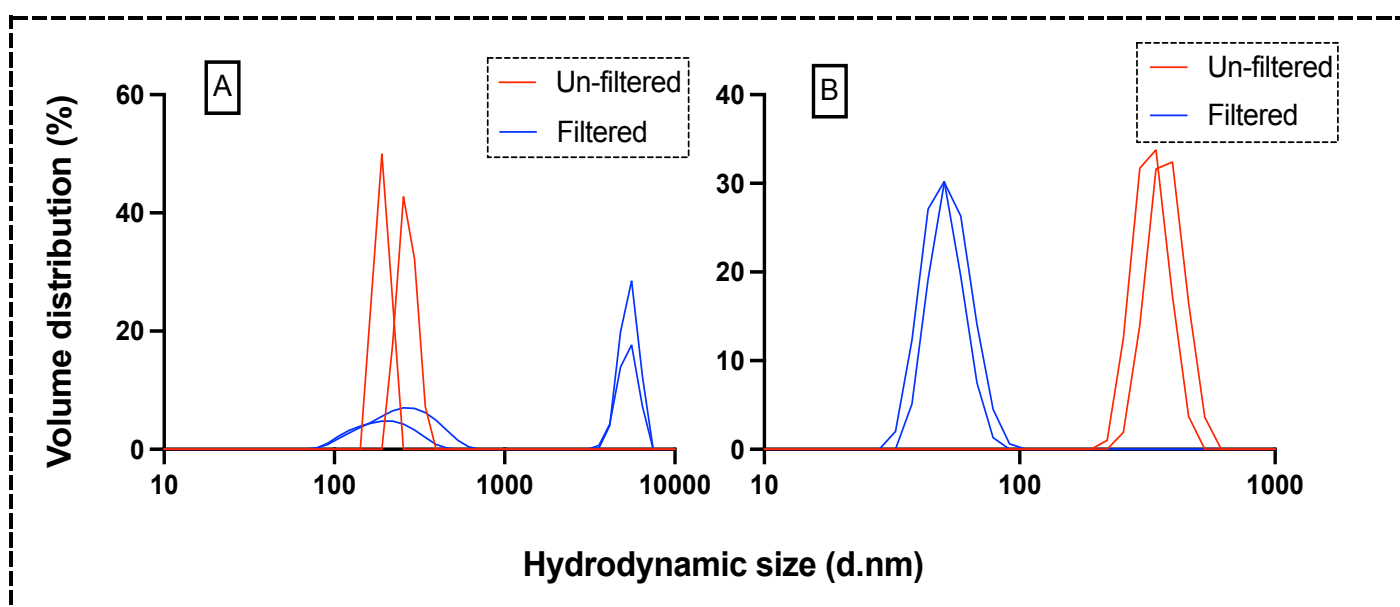


Figure (A2): Aggregation of A33 hFab' in isopropyl alcohol shown by dynamic light scattering method. Plot (A2-A) represents multiple measurements of the filtered and

un-filtered samples using 173° backscatter angle and (A2-B) clarifying the multiple measurements of the filtered and un-filtered sample using 13° forwardscatter angle.